

000 CONVREC-R1: TRAINING LLM-BASED CONVERSATIONAL 001 RECOMMENDER SYSTEMS WITH REINFORCEMENT LEARNING 002

003 **Anonymous authors**
004

005 Paper under double-blind review
006

007 ABSTRACT 008

009 Large language models (LLMs) are reshaping the recommender system paradigm
010 by enabling users to express preferences and receive recommendations through
011 conversations. Yet, aligning LLMs to the recommendation task remains challeng-
012 ing: pretrained LLMs often generate out-of-catalog items, violate required output
013 formats, and their ranking quality degrades sharply toward the end of the generated
014 list. To this end, we propose **ConvRec-R1**, a two-stage framework for end-to-end
015 training of LLM-based conversational recommender systems. In Stage 1, we con-
016 struct a behavioral-cloning dataset with a *Remap-Reflect-Adjust* pipeline, which
017 produces high-quality, catalog-grounded demonstrations from powerful blackbox
018 LLMs to warm-start the RL training. In Stage 2, we propose **Rank-GRPO**, a
019 principled extension of group relative policy optimization (GRPO) (Shao et al.,
020 2024) tailored to tasks with rank-style outputs. Rank-GRPO treats each rank in
021 the recommendation list as the unit instead of token (*too fine-grained*) or sequence
022 (*too coarse*), redefining rewards to remove non-causal credit assignment and in-
023 troducing a rank-level importance ratio based on the geometric mean of rank-
024 wise token probabilities to stabilize policy updates. Experiments on the public
025 REDDIT-V2 dataset show that ConvRec-R1 converges faster and achieves higher
026 Recall and NDCG than GRPO-style baselines. Code and datasets are released at
027 [028 https://anonymous.4open.science/r/ConvRec-R1-5615/](https://anonymous.4open.science/r/ConvRec-R1-5615/).
029

030 1 INTRODUCTION 031

032 Recommender systems (RS) are undergoing a fundamental shift in the era of generative AI. Instead
033 of passively predicting user behaviors, the emerging conversational RSs (CRS) paradigm position
034 themselves as proactive agents that allow users to articulate nuanced preferences and receive tailored
035 recommendations through interactive dialogue (Zhang et al., 2024). Large language models (LLMs)
036 are at the center of this transformation: Their broad knowledge and reasoning capabilities enable
037 both preference understanding and recommendation generation directly from user queries. Unlike
038 earlier LLM-based RS that embed item ID tokens into the LLM (Hua et al., 2023), recent studies
039 emphasize the benefits of representing items in natural language (He et al., 2023; Zhu et al., 2025).
040 This representation not only preserves the LLM’s core language capability but also provides flexi-
041 bility to verbally guide CRS toward different recommendation objectives, such as novelty, diversity,
042 or emotion-oriented relevance, while seamlessly integrating recommendation functionality.
043

044 Despite this promise, aligning LLMs with real-world recommendation tasks remains challenging,
045 primarily due to the following three key limitations. First, trained on general web datasets, LLMs
046 inherently lack awareness of item catalog specific to a given platform (e.g., the full set of TV shows
047 available on streaming service platforms). Without explicit catalog grounding, they frequently gen-
048 erate out-of-catalog or even non-existent items in a zero-shot manner, severely limiting their prac-
049 tical utility. Second, LLMs often fail to conform to predefined output formats for the items (e.g.,
050 including both the title and release year for movies), which complicates item matching and inte-
051 gration with downstream systems. Third, the quality of generated recommendation lists deteriorates
052 sharply toward the end, due to the scarcity of high-quality ranking-style data in the pretraining stage.
053 These challenges are particularly severe for smaller LLMs, which are less powerful but commonly

054 adopted in practice to meet industrial-level efficiency and latency constraints. Collectively, the above
 055 limitations present significant barriers to the deployment of LLM-based CRS in real-world settings.
 056

057 Recently, reinforcement learning from verifiable reward (RLVR) (Lambert et al., 2024) offers a
 058 promising direction for alignment, as it introduces structured rewards that can explicitly guide LLMs
 059 toward generating catalog-grounded, high-quality recommendation lists. However, applying RL to
 060 LLM-based CRS presents two fundamental challenges. First, since RLVR relies on self-exploration
 061 for policy update, a warm-start behavior cloning stage with high-quality human demonstrations is
 062 generally required beforehand to ensure efficiency and stability (Shao et al., 2024; Zhu et al., 2024a;
 063 Wei et al., 2025). Yet it is impractical to expect human annotators to produce large-scale catalog-
 064 grounded item lists with good rankings, both due to the difficulty of recalling a large and dynamic
 065 catalog and the influence of subjective biases. Furthermore, prevalent RLVR algorithms such as
 066 group relative policy optimization (GRPO) (Shao et al., 2024; Yu et al., 2025; Liu et al., 2025) are
 067 **fundamentally misaligned** with tasks with rank-style outputs. These methods typically conduct
 068 token-wise policy updates based on sequence-level rewards. However, sequence-level rewards (e.g.,
 069 the overall NDCG of a recommendation list) are too coarse to capture the contribution of individual
 070 items in each rank, while token-level updates are overly fine-grained as each item can be represented
 071 by multiple tokens. This mismatch leads to non-causal credit assignment, misaligned importance
 072 weighting, unstable policy optimization, and ultimately poor quality in generated recommendations.
 073

074 To address these challenges, we propose **ConvRec-R1**, a novel two-stage framework for end-to-end
 075 training of LLM-based CRS. Specifically, in Stage 1, we design a lightweight distillation pipeline,
 076 *Remap–Reflect–Adjust*, which leverages zero-shot recommendations from a powerful teacher LLM
 077 on training conversations to construct catalog-grounded demonstrations for supervised fine-tuning
 078 (SFT). Specifically, teacher-generated recommendation lists are first projected into the target catalog
 079 space (*Remap*), then refined with contextual judgments to improve ranking quality (*Reflect*), and
 080 finally corrected for residual popularity biases relative to training distributions (*Adjust*). This process
 081 establishes exemplar demonstrations of high-quality ranked items for training conversations, which
 082 warm-starts the LLM with catalog awareness, proper item formatting, and initial ranking ability
 083 before subsequent RL post-training. Furthermore, in Stage 2, we develop **Rank-GRPO**, a principled
 084 extension of GRPO designed for tasks with rank-style outputs, where user feedback can be treated
 085 as verifiable reward. Rank-GRPO considers each rank as the unit for both advantage estimation
 086 and importance reweighting, introducing reward masking to prevent non-causal credit assignment
 087 and defining a rank-level importance ratio via the geometric mean of item token probabilities to
 088 stabilize policy updates. Experiments on the public REDDIT-v2 dataset demonstrate that ConvRec-
 089 R1 substantially improves the recommendation quality over zero-shot LLMs, converges faster and
 090 achieves superior Recall and NDCG in recommendations than GRPO-style baselines.
 091

092 2 METHODOLOGY

093 2.1 PROBLEM FORMULATION

094 In this paper, we formulate conversational recommendation as a sequential decision problem. Given
 095 a dialogue between a user and the system $x = (x_1, \dots, x_{T_x})$ composed of T_x tokens, the goal is to
 096 learn a policy $\pi_\theta(y|x)$, parameterized by a target LLM with learnable parameters θ , that generates
 097 a ranked list of N items $y = (y^{(1)}, y^{(2)}, \dots, y^{(N)})$ as recommendations. Here, we note that each
 098 item $y^{(k)} = (y_1^{(k)}, \dots, y_{L_k}^{(k)})$ is itself a sequence of tokens represented in natural language (e.g.,
 099 a movie title with release year), rather than a numerical identifier in traditional RS. Ideally, each
 100 selected item should belong to a predefined item catalog, i.e., $y^{(k)} \in \mathcal{C}$. The generation process
 101 of y can be decomposed into a sequence of N rank-wise decisions. At each rank k , the policy
 102 generates the next item $y^{(k)}$ conditioned on the context x and the previously generated items $y^{(<k)} =$
 103 $(y^{(1)}, \dots, y^{(k-1)})$. During generation, we instruct the LLM-based policy π_θ to separate items in the
 104 recommendation list y with a special delimiter (e.g., a newline token $\backslash n$) as follows:

$$y_{\text{text}} = [y^{(1)} \oplus \backslash n \oplus y^{(2)} \oplus \dots \oplus y^{(N)} \oplus \text{<eos>}], \quad (1)$$

105 where \oplus denotes concatenation and <eos> marks the end of the generation process. To simplify
 106 the notation, we absorb $\backslash n$ with the previous item (and <eos> for the last item) and use y and y_{text}
 107 interchangeably. The LLM-based π_θ generates this sequence y auto-regressively at the token level.

108
109

2.2 SUPERVISED FINE-TUNING

110 The **Stage 1** of the ConvRec-R1 framework is **supervised fine-tuning (SFT)**, which aims to warm-
 111 start the LLM-based CRS policy $\pi_\theta(y|x)$ with the foundational knowledge of the item catalog,
 112 required output formats, and the ability to generate and rank lists of items for recommendations. To
 113 address the critical challenge of lacking high-quality in-catalog item ranking data, we construct a
 114 behavior cloning dataset, $\mathcal{D}_{\text{SFT}} = \{(x_i^{\text{SFT}}, y_i^{\text{SFT}})\}_{i=1}^M$ by distilling exemplar catalog-grounded
 115 recommendation demonstrations y_i^{SFT} for training conversations x_i^{SFT} from a powerful teacher LLM
 116 (e.g., GPT-4o), which is often infeasible for direct deployment due to high costs and latency.

117

118 2.2.1 TEACHER-GENERATED PRELIMINARY DEMONSTRATIONS

119 The distillation process begins by generating a zero-shot list of N candidate items for each dialogue
 120 x_i^{SFT} in the SFT training set. This is achieved by prompting a powerful teacher LLM Θ to produce
 121 a preliminary item list $y_{i,\text{raw}}^{\text{SFT}} \sim \pi_\Theta(y|x_i^{\text{SFT}})$, following the same structure as Eq. (1). The items and
 122 ranks in $y_{i,\text{raw}}^{\text{SFT}}$ benefit from the teacher’s advanced knowledge and reasoning ability, which represents
 123 the state of the art in open-item recommendations (He et al., 2023; Zhu et al., 2025). However, these
 124 recommendations lie within the teacher’s own recommendation space \mathcal{C}_Θ ,¹ which is not necessarily
 125 aligned with the target catalog \mathcal{C} . Consequently, $y_{i,\text{raw}}^{\text{SFT}}$ may still include out-of-catalog (OOC) items,
 126 minor formatting inconsistencies, or rankings with the teacher’s internal biases.

127

128 2.2.2 THE REMAP-REFLECT-ADJUST PIPELINE

129 To correct these misalignments, we refine the teacher’s raw recommendations $y_{i,\text{raw}}^{\text{SFT}}$ through a three-
 130 step *Remap–Reflect–Adjust* pipeline. This process calculates a score $s_{\text{final}} \in \mathbb{R}^{|\mathcal{C}|}$ over all items in
 131 the catalog \mathcal{C} , which is then ranked to produce the demonstration y_i^{SFT} (see Appendix A for details).

132 **(i) Remap.** This step grounds the teacher’s recommendations by mapping them from the teacher’s
 133 recommendation space \mathcal{C}_Θ into the target catalog space \mathcal{C} . Specifically, we compute an initial score
 134 $s_{\text{remap}} \in \mathbb{R}^{|\mathcal{C}|}$ using the aggregation: $s_{\text{remap}} = \mathbf{p} \cdot (S_{\text{item-item}} + \mathbf{I}_{\text{ic}}) + \lambda \cdot s_{\text{conv-item}}$. Here, $\mathbf{p} \in$
 135 $\mathbb{R}^{|\mathcal{C}_\Theta|}$ is a sparse vector where non-zero entries represent the positional scores of items in $y_{i,\text{raw}}^{\text{SFT}}$,
 136 heuristically calculated as $1/\sqrt{k}$ for the item at rank k . The item-item similarity matrix $S_{\text{item-item}} \in$
 137 $\mathbb{R}^{|\mathcal{C}_\Theta| \times |\mathcal{C}|}$ maps each item from \mathcal{C}_Θ to the target catalog \mathcal{C} based on semantic similarity, where $\mathbf{I}_{\text{ic}} \in$
 138 $\{0, 1\}^{|\mathcal{C}_\Theta| \times |\mathcal{C}|}$ is a sparse indicator mapping matrix with $I_{\text{ic}}[u, v] = 1$ iff the u -th item in \mathcal{C}_Θ equals
 139 the v -th catalog item, which directly transfers scores for in-catalog items. Finally, $s_{\text{conv-item}} \in \mathbb{R}^{|\mathcal{C}|}$
 140 encodes the content similarity between the dialogue x_i^{SFT} and in-catalog items.

141 **(ii) Reflect.** While the remapping step grounds $y_{i,\text{raw}}^{\text{SFT}}$ to scores in the catalog space, the ranking
 142 quality based on semantic similarity can be further improved. In the *reflect* step, we use LLM-as-a-
 143 judge to enhance the contextual relevance by asking the same teacher LLM to rate candidates with
 144 top- $N_r > N$ remapped scores s_{remap} on a numerical scale from $-L$ (worst) to $+L$ (best) based on
 145 their suitability as recommendations for the context x_i^{SFT} . These raw ratings are then normalized to
 146 form a sparse vector $\mathbf{r}_{\text{reflect}} \in \mathbb{R}^{|\mathcal{C}|}$, which is scaled by a weight γ and added to the remapped scores
 147 to produce a context-enhanced refined score vector as: $s_{\text{reflect}} = s_{\text{remap}} + \gamma \cdot \mathbf{r}_{\text{reflect}}$.

148 **(iii) Adjust.** The reflected scores already provide a strong basis for ranking, but the final *adjust*
 149 step can further correct for residual popularity biases inherited from the teacher model. Specifically,
 150 we align the scores with the empirical distribution of the groundtruth items in the training data by
 151 learning an item-specific multiplicative bias $\mathbf{w} \in \mathbb{R}^{|\mathcal{C}|}$ and an additive bias $\mathbf{b} \in \mathbb{R}^{|\mathcal{C}|}$, where the
 152 final score is computed as $s_{\text{final}} = \mathbf{w} \odot s_{\text{reflect}} + \mathbf{b}$, where \odot denotes the Hadamard (element-wise)
 153 product. The final demonstration list y_i^{SFT} can then be constructed by selecting the top- N items from
 154 the catalog \mathcal{C} according to their scores in s_{final} and formatting them as the structured textual string
 155 shown in Eq. (1). With the established SFT dataset \mathcal{D}_{SFT} , the objective of behavior cloning can be
 156 formalized as minimizing the negative log-likelihood of the demonstrations as follows:

$$\mathcal{L}_{\text{SFT}}(\theta) = -\mathbb{E}_{(x_i^{\text{SFT}}, y_i^{\text{SFT}}) \sim \mathcal{D}_{\text{SFT}}} [\log \pi_\theta(y_i^{\text{SFT}} | x_i^{\text{SFT}})]. \quad (2)$$

160
 161 ¹Since the training conversations in \mathcal{D}_{SFT} are fixed, the teacher’s recommendation space \mathcal{C}_Θ is defined as
 the union of all unique items generated by the teacher LLM Θ for these conversations.

162 2.3 REINFORCEMENT LEARNING-BASED ALIGNMENT
163

164 After the initial SFT stage, we further align the LLM-based CRS policy $\pi_{\theta_{\text{SFT}}}(y|x)$ (hereafter, sub-
165 script $_{\text{SFT}}$ will be omitted for brevity) using reinforcement learning (RL), optimizing it directly
166 against the structured reward derived from user feedback. We use $\mathcal{D}_{\text{RL}} = \{(x_i^{\text{RL}}, y_i^{\text{gt}})\}_{i=1}^{M_{\text{RL}}}$ to de-
167 note the training data in the RL phase, where x_i^{RL} is a training conversation and $y_i^{\text{gt}} \subseteq \mathcal{C}$ is the set of
168 in-catalog items that the user provided positive feedback after the conversation.

169 2.3.1 VANILLA GRPO
170

171 In this paper, we mainly focused on the prevalent RL alignment method, group relative policy op-
172 timization (GRPO) (Shao et al., 2024), which leverages the relative rewards among a group of re-
173 sponses to estimate advantage and eliminate the need for a learned value model (Schulman et al.,
174 2017). For each dialogue $x_i^{\text{RL}} \in \mathcal{D}_{\text{RL}}$, GRPO first generates a group of G responses $\{y_i\}_{i=1}^G$ from
175 a sampling policy $\pi_{\theta_{\text{old}}}(y|x)$, where θ_{old} is typically the model μ update-steps before θ . Under the
176 setting of CRS, each y_i is a ranked list of N items, i.e., $y_i = (y_i^{(1)}, \dots, y_i^{(N)})$, which is evaluated
177 against the groundtruth y_i^{gt} to calculate a reward score reflecting its overall quality. Based on the
178 relative rewards across the G generations in the group, GRPO estimates a low-variance advantage
179 for each response \hat{A}_i , which can be used to update the policy by maximizing the following objective:
180

$$181 \mathcal{J}_{\text{GRPO}}(\theta) = \mathbb{E}_{x \sim \mathcal{D}_{\text{RL}}, \{y_i\}_{i=1}^G \sim \pi_{\theta_{\text{old}}}(\cdot|x)} \left[\frac{1}{G} \sum_{i=1}^G \frac{1}{|y_i|} \sum_{t=1}^{|y_i|} \min \left(w_{i,t}(\theta) \hat{A}_{i,t}, \text{clip}(w_{i,t}(\theta), 1 - \epsilon, 1 + \epsilon) \hat{A}_{i,t} \right) \right], \quad (3)$$

184 where the importance ratio $w_{i,t}(\theta)$ and advantage $\hat{A}_{i,t}$ for each token $y_{i,t}$ are:
185

$$186 w_{i,t}(\theta) = \frac{\pi_{\theta}(y_{i,t}|x, y_{i,<t})}{\pi_{\theta_{\text{old}}}(y_{i,t}|x, y_{i,<t})}, \quad \hat{A}_{i,t} = \hat{A}_i = \frac{r(x, y_i) - \text{mean}(\{r(x, y_i)\}_{i=1}^G)}{\text{std}(\{r(x, y_i)\}_{i=1}^G)}.$$

188 We omit the KL-divergence with base policy (i.e., the SFT model θ_{SFT}) in Eq. (3) for readability.
189 Here, the importance sampling term $w_{i,t}(\theta)$ allows unbiased advantage estimate with samples gener-
190 ated from the old policy $\pi_{\theta_{\text{old}}}$. To facilitate stable updates, the objective function clips the importance
191 ratio, limiting how far the new policy can diverge from $\pi_{\theta_{\text{old}}}$. The sequence-level reward $r(x, y_i)$ is
192 typically a ranking-based metric such as DCG@ N , defined as $\sum_{k=1}^N \frac{\text{rel}_k}{\log_2(k+1)}$. The relevance score
193 rel_k is 1 if the item $y_i^{(k)}$ at rank k is in the groundtruth set y_i^{gt} and has not appeared at an earlier rank;
194 the relevance is 0 for all other cases, including repeated, non-relevant, and out-of-catalog items.
195

196 **Gradient Analysis and Limitations.** Although GRPO has shown effectiveness in many other do-
197 mains with verifiable rewards, such as math problem solving (Guo et al., 2025) and code generation
198 (Zhu et al., 2024a), the gradient analysis of its unclipped objective (for simplicity) reveals **two fun-
199 damental misalignments** when applied to ranking tasks (see Appendix B for derivation):

$$200 \nabla_{\theta} \mathcal{J}_{\text{GRPO}}(\theta) \propto \mathbb{E} \left[\sum_{i=1}^G \frac{1}{|y_i|} \sum_{t=1}^{|y_i|} \underbrace{w_{i,t}(\theta)}_{\text{token (}t\text{-level importance ratio}} \cdot \underbrace{\hat{A}_i}_{\text{sequence (}i\text{-level advantage}} \cdot \underbrace{\nabla_{\theta} \log \pi_{\theta}(y_{i,t}|x, y_{i,<t})}_{\text{token (}t\text{-level gradient of log-likelihood}} \right]. \quad (4)$$

204 Intuitively, Eq. (4) shows that maximizing Eq. (3) increases or decreases the log-likelihood of each
205 token in the generated response y_i according to the sign of the advantage (scaled by the importance
206 weight). However, (i) for the ranking task, the sequence-level reward $r(x, y_i)$ (e.g., DCG@ N of the
207 whole list) is assigned uniformly to every token, leading to *non-causal credit assignment*: tokens in
208 the later items inherit reward from earlier ranks, but the auto-regressive generation goes the other
209 way around. Take the DCG reward as an example, we note that it can be naturally decomposed as a
210 sum of temporally discounted rank-level rewards (i.e., the relevance rel_k here) as follows:
211

$$212 \text{DCG}@N = \sum_{j=1}^N \frac{\text{rel}_j}{\log_2(j+1)} \triangleq \sum_{j=1}^N \frac{\text{reward}_j}{\text{discount}_j} = \underbrace{\sum_{j=1}^{k-1} \frac{\text{reward}_j}{\log_2(j+1)}}_{\text{non-causal for item at rank } k} + \underbrace{\sum_{j=k}^N \frac{\text{reward}_j}{\log_2(j+1)}}_{\text{causal for item at rank } k}. \quad (5)$$

214 Here, tokens of item at rank k not only take credit for itself and items recommended afterwards, but
215 also from previous recommendations. This becomes especially problematic toward the end of the

list (i.e., when k is close to N), as the recommendation quality deteriorates significantly, but they accumulate credit from strong recommendations at front ranks. Moreover, **(ii)**, in the off-policy step where $\mu > 0$, the token-level importance ratio is too fine-grained and mismatched with sequence-level advantages. Recent methods such as group sequence policy optimization (GSPO) (Zheng et al., 2025) mitigate the mismatch with sequence-level importance weights, yet they remain misaligned for the ranking task, as each rank should be the natural action unit instead of the whole sequence.

2.3.2 RANK-GRPO

To address the misalignment of vanilla GRPO and GSPO, we propose **Rank-GRPO**, a principled RL alignment algorithm for tasks with rank-structured outputs (e.g., recommendations). The core insight is to treat each rank as a distinct action unit instead of a token (*too fine-grained*) or a sequence (*too coarse*), which enables a more precise and rank-aware credit assignment and importance weighting for policy updating. Here, another major challenge is that computing the true advantage for an item at rank k would, in principle, require enumerating trajectories that share the same prefix items $y^{(<k)}$, which grows combinatorially. To address this, Rank-GRPO adopts a *rank-wise advantage estimation* based on the same G trajectories used in GRPO, reducing complexity from exponential to linear while retaining effectiveness. The objective of Rank-GRPO is defined as:

$$\mathcal{J}_{\text{Rank-GRPO}}(\theta) = \mathbb{E}_{x \sim \mathcal{D}_{\text{RL}}, \{y_i\}_{i=1}^G \sim \pi_{\theta_{\text{old}}}(\cdot|x)} \left[\frac{1}{GN} \sum_{i=1}^G \sum_{k=1}^N \min(w_{i,k}(\theta) \hat{A}_{i,k}, \text{clip}(w_{i,k}(\theta), 1-\epsilon, 1+\epsilon) \hat{A}_{i,k}) \right], \quad (6)$$

where the rank-level importance ratio $w_{i,k}(\theta)$ and advantage $\hat{A}_{i,k}$ are defined as:

$$w_{i,k}(\theta) = \frac{\bar{\pi}_{\theta}(y_i^{(k)}|x)}{\bar{\pi}_{\theta_{\text{old}}}(y_i^{(k)}|x)}, \quad \hat{A}_{i,k} = \frac{r(x, y_i^{(k)}) - \text{mean}_{i'}[r(x, y_{i'}^{(k)})]}{\text{std}_{i'}[r(x, y_{i'}^{(k)})]}, \text{ where}$$

$$\bar{\pi}_{\theta}(y_i^{(k)}|x) = \left(\prod_{t=1}^{|y_i^{(k)}|} \pi_{\theta}(y_{i,k,t}|x, y_{i,k,<t}) \right)^{1/|y_i^{(k)}|} = \exp \left(\frac{1}{|y_i^{(k)}|} \sum_{t=1}^{|y_i^{(k)}|} \log \pi_{\theta}(y_{i,k,t}|x, y_{i,k,<t}) \right).$$

We again omit the KL-divergence with the SFT base policy in Eq. (6) for readability (like in Eq. (3)). Here, $\bar{\pi}_{\theta}(y_i^{(k)}|x)$ denotes the *effective probability* for rank- k , which is defined as the geometric mean of the token probabilities for the item at the k -th rank. This normalization ensures stable importance weights across items with varying token lengths. The rank-wise advantage $\hat{A}_{i,k}$ is derived from a *rank-level return* $r(x, y_i^{(k)})$ that evaluates both the immediate reward (quality) of the item at rank k and its downstream influence on subsequent recommendations from rank $k+1$ through N .

Gradient Analysis and Insights. Before delving into the specific form of the rank-level return $r(x, y_i^{(k)})$, we first analyze the gradient of Rank-GRPO and demonstrate that it effectively addresses the two fundamental misalignments of vanilla GRPO on rank-structured outputs. The policy gradient for Rank-GRPO (Here we also consider the unclipped objective like Eq. (4) for simplicity) highlights its rank-centric policy update mechanism (see Appendix B for the derivation):

$$\begin{aligned} \nabla_{\theta} \mathcal{J}_{\text{Rank-GRPO}}(\theta) &\propto \mathbb{E} \left[\sum_{i=1}^G \sum_{k=1}^N w_{i,k}(\theta) \hat{A}_{i,k} \nabla_{\theta} \log \bar{\pi}_{\theta}(y_i^{(k)}|x) \right] \\ &= \mathbb{E} \left[\sum_{i=1}^G \sum_{k=1}^N \underbrace{w_{i,k}(\theta)}_{\text{rank } (k)\text{-level importance ratio}} \cdot \underbrace{\hat{A}_{i,k}}_{\text{rank } (k)\text{-level advantage}} \cdot \underbrace{\frac{1}{|y_i^{(k)}|} \sum_{t=1}^{|y_i^{(k)}|} \nabla_{\theta} \log \pi_{\theta}(y_{i,k,t}|x, y_{i,k,<t})}_{\text{rank } (k)\text{-level gradient of log-likelihood}} \right]. \end{aligned} \quad (7)$$

The formulation in Eq. (7) shows that Rank-GRPO fundamentally resolves the issues of vanilla GRPO: First, instead of applying a uniform sequence-level reward to every token, we assign a *rank (k)-specific advantage* $\hat{A}_{i,k}$ for all the tokens of items at the k -th rank, ensuring that all tokens of the k -th item are updated consistently based on its contribution. Second, the importance weight and the gradient also operate at the rank level, where the effective probability $\bar{\pi}_{\theta}(y_i^{(k)}|x)$ aggregates token-level information for each rank, thereby improving the stability for policy updates.

2.3.3 REWARD SHAPING

Following the analysis of the sequence-level DCG@ N reward as Eq.(5), in Rank-GRPO, we define the rank (k)-level return $r(x, y_i^{(k)})$ by masking out the “non-causal part” in DCG@ N and keeping only the “causal part”, which we denote as DCG@ $k:N$ as follows:

$$r(x, y_i) \triangleq \text{DCG}@N = \sum_{j=1}^N \frac{\text{rel}_j}{\log_2(j+1)} \longrightarrow r(x, y_i^{(k)}) \triangleq \text{DCG}@k:\text{N} = \sum_{\substack{j=k}}^N \frac{\text{rel}_j}{\log_2(j+1)}. \quad (8)$$

DCG@ $k:N$ ensures each item $y_i^{(k)}$ receives credit only for its own contribution, respecting the sequential generation from higher rank to lower rank where earlier decisions influence the later ones. Although DCG@ $k:N$ minimally adapts the metric of interest (NDCG@ N), it is not necessarily the best reward for generative retrieval tasks, as the most influence of each item generation should come from the user query x as context compared to the already-generated items in the higher ranks $y_i^{(<k)}$. Therefore, we introduce an exponential decay variant of reward for Rank-GRPO as follows:

$$r_{\exp_\Gamma}(x, y_i^{(k)}) \triangleq \sum_{j=k}^N \frac{\text{rel}_j}{\Gamma^{(j-k)}} = \text{rel}_k + \frac{1}{\Gamma} \cdot r_{\exp_\Gamma}(x, y_i^{(k+1)}), \quad (9)$$

where $\Gamma > 1$ controls the discount rate. In the limit $\Gamma = \infty$, only the current item's relevance is credited. In practice, we find that $\Gamma = \infty$ provides a simple, stable and effective learning signal. We distinguish the two Rank-GRPO variants with the rank-wise return defined in Eqs. (8) and (9) as Rank-GRPO (log) and Rank-GRPO (\exp_∞), respectively.

To further stabilize RL training, we add two penalties for instruction-following failures:

- (i) **Incomplete Lists.** If the model generates fewer than N items before emitting an `<eos>` token ($N_o < N$), the missing ranks are treated as irrelevant (zero return), and the premature stop token in this rollout receives a penalty $\epsilon_o < 0$ to discourage under-generation.
- (ii) **Overflow Items.** If the model generates more than N items, each overflow item beyond rank N receives a penalty $\epsilon_o < 0$ to discourage over-generation despite explicit instructions.

Although more sophisticated reward shaping methods are possible (e.g., using sliding-window constraints on the horizon of the return), as the first rank-aware RL alignment framework, we find that Eqs. (8) and (9) are effective in practice and leave these extensions to future work.

3 EXPERIMENTS

3.1 DATASETS

In the main paper, we focus on the REDDIT-v2 dataset, the largest publicly available benchmark for CRS ($\sim 400k$) that could support LLM post-training (He et al., 2023; Zhu et al., 2025). REDDIT-v2 consists of multi-turn dialogue sessions in which users mention or request movies, paired with groundtruth items that received positive feedback during the conversation. Following the protocol of He et al. (2023) and Zhu et al. (2025), the dataset is split into training, validation, and test sets with 383,013, 9,421, and 10,972 conversations. One notable difference with prior work is that we also require the LLM to output the *release year together with the title* for each recommendation, which is more difficult but important for disambiguation and catalog matching. To construct our supervised fine-tuning (SFT) dataset, we apply the *Remap–Reflect–Adjust* pipeline to 25% of the training set and the entire validation set (for monitoring). This produces a catalog-grounded behavior cloning dataset \mathcal{D}_{SFT} that serves to warm-start the RL phase and is released along with trained SFT checkpoints to facilitate future research. The full experiments on the REDDIT-v2 dataset are reported in Appendix D.7.

3.2 IMPLEMENTATION

We evaluate ConvRec-R1 with three open-source instruction-tuned LLMs as the backbone models: Qwen2.5-0.5B-Instruct, Llama-3.2-1B-Instruct, and Llama-3.2-3B-Instruct, as models larger than 3B may introduce higher latency and computational overhead, which pose significant challenges for

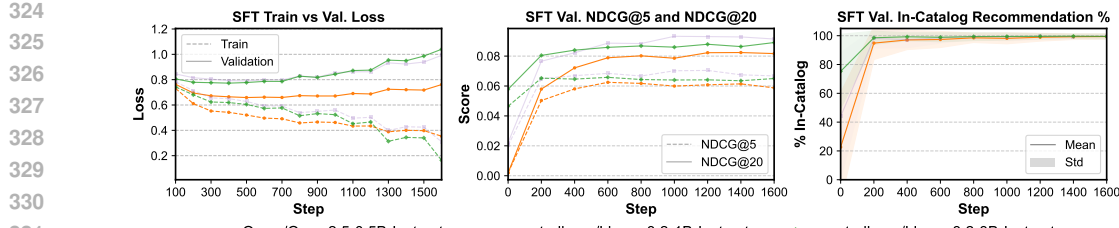


Figure 1: Training dynamics on loss, validation metrics, validation in-catalog recommendation ratio with different backbone models during the **SFT** stage on the REDDIT-V2 dataset.

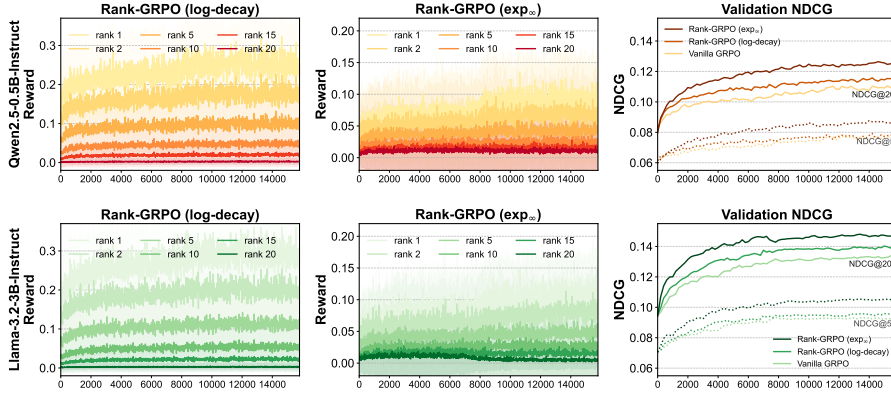


Figure 2: **Left + Middle**: Training dynamics of the reward acquired by ConvRec-R1 with Rank-GRPO on different rank during the **RL** stage. **Right**: Comparison of validation NDCG between GRPO and Rank-GRPO (both on-policy) on the REDDIT-V2 dataset.

their practical deployment. More details on the implementation and hyperparameters are provided in Appendix C. We also provide the detailed establishment process of the SFT dataset, the exact prompt templates used for the *reflect* step and recommendation, additional experimental studies, and qualitative analyses on generations in Appendix A, D and F, respectively.

3.3 EVALUATION OF THE SFT STAGE

In Sections 3.3 and 3.4, we analyze training dynamics on the **train/validation** sets, while test set evaluation is deferred to Section 3.5. During the SFT stage, we observe *three key phenomena* in Fig. 1. First, while training loss decreases steadily, validation loss plateaus around 800 steps², reflecting the difficulty of learning long, structured recommendation lists purely through behavior cloning. Second, the high-quality SFT data provides a strong initialization by grounding the model in the catalog and enforcing output format, where the proportion of in-catalog recommendations rapidly surpasses 99% across backbones. Third, the ranked list generation ability improves drastically over the initial zero-shot model, with NDCG@20 increasing over **30×**, **3×**, and **1.5×** for the **0.5B**, **1B**, and **3B** model, respectively. Overall, SFT is crucial for warming up the models, i.e., constraining them to the catalog, ensuring proper formatting, and improving long list generation ability before RL, which improves both sampling efficiency (for self-exploration) and training stability.

3.4 EVALUATION OF THE RL STAGE

We then analyze the training dynamics of ConvRec-R1 in the RL stage. Figures 2 and 3 show the rewards obtained at different ranks in the generated recommendation list on the training set. From the figures we observe that during training with **Rank-GRPO**, rewards increase monotonically across ranks in both on-policy and off-policy settings. Figures 2 and 3-(right) further report the dynamics of NDCG on the validation set. Compared to GRPO and GSPO (in the off-policy setting, as both are the same in the on-policy setting), Rank-GRPO converges faster and achieves higher NDCG, with

²Nevertheless, we adopt the 1,500-step SFT checkpoint for RL for stronger catalog memory. Starting with the InstructGPT (Ouyang et al., 2022), it is common to initialize RL from slightly overfitted SFT model.

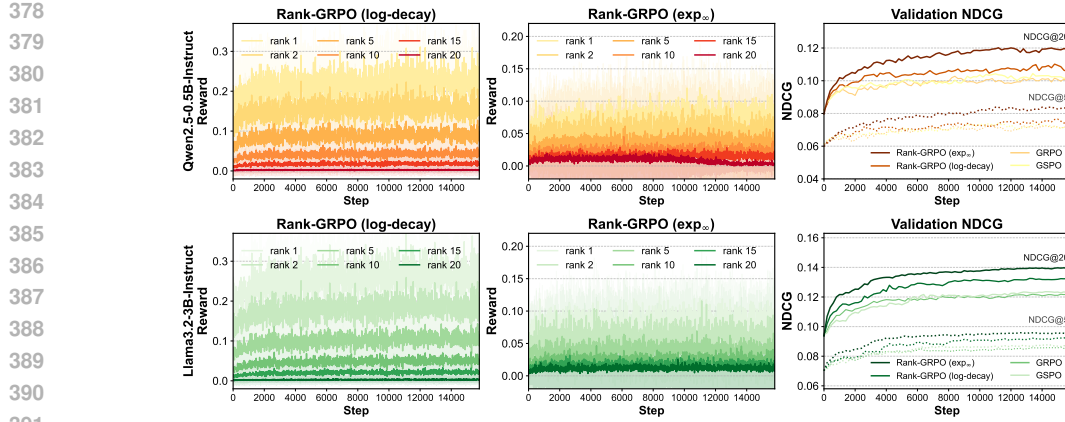


Figure 3: Training dynamic of reward and validation NDCG between GRPO, GSPO and Rank-GRPO (off-policy) on REDDIT-V2. See Appendix Fig. 5 for results with Llama3.2-1B-Instruct.

particularly larger improvements with large k . This suggests that the generated recommendation sequences with Rank-GRPO-trained LLM not only improve in overall quality but also maintain good quality toward the tail of the list, where standard methods typically degrade. Theoretically, differences in reward between GRPO and Rank-GRPO at the front ranks are relatively small (e.g., for both sequence-level DCG@ N and rank-level DCG@ $1:N$, rewards on the first item are identical, see Eq. (8)), while improvements accumulate more substantially at later positions. In contrast, Rank-GRPO (\exp_∞) significantly improves the performance at higher ranks, demonstrating the major influence of context on recommendations compared to the items generated in the higher ranks. Another interesting phenomenon we observed from the training dynamic of Rank-GRPO (\exp_∞) (see the middle plots in Figures 2 and 3) is that the relevance (reward) of recommendations generated at lower ranks (e.g., 15, 20, represented by the darker lines) increases and then decreases as the training proceeds, while the relevance of recommendations generated at higher ranks (e.g., 1, 2, 5 represented by the lighter lines) increases monotonically in trend. This is interesting as it shows the RL alignment stage of Rank-GRPO (\exp_∞) resembles a retrieval and rerank strategy where relevant items are first included in the generated list and then moved to higher ranks motivated by the reward.

In addition, the improvement is also evident in the off-policy setting where we set the per-sampling policy update step $\mu = 2$ (Figure 3), which demonstrates the advantage of Rank-GRPO over GRPO and GSPO by aligning rank-wise importance weights with rank-wise rewards. We also note that off-policy performance at the same step lags behind on-policy performance due to the higher variance introduced by importance weighting, though the ability to reuse trajectories sampled by previous policies offers a favorable trade-off in efficiency. Due to space limits, we present results for Qwen2.5-0.5B-Instruct (on/off policy) and Llama3.2-3B-Instruct (on policy) in the main text. The full experiments with the remaining LLM backbones are reported in Appendix D.4.

3.5 COMPARISON WITH BASELINES

Finally, we present the one-time evaluation on the test set, which is collected one month after the validation set (He et al., 2023; Zhu et al., 2025). We compare different backbone LLMs trained with ConvRec-R1 with state-of-the-art CRSs, including training-based methods and prompting-based black-box LLMs. The detailed description of baselines is provided in Appendix D.2. From Table 1, we observe that both stages of ConvRec-R1 contribute substantially to its superior performance over the baselines. The **SFT** stage provides a strong boost over the zero-shot baseline by grounding the recommendations in the catalog with the correct format, which improves the efficiency and stability of the RL training. The **RL** stage further enhances performance, especially at higher ranks, by aligning generation with rank-wise rewards. With these improvements, ConvRec-R1 with Qwen2.5-0.5B-Instruct backbone substantially outperforms GPT-4o-mini, ConvRec-R1 with Llama3.2-1B-Instruct backbone performs on par with GPT-4o, and ConvRec-R1 with Llama3.2-3B-Instruct backbone even surpasses GPT-4o and CRAG (GPT-4o) on recall/NDCG@20. Notably, CRAG requires 5–7 GPT-4o API calls per recommendation (for mentioned item extraction, reflection, and re-ranking), incurring far higher cost and latency, whereas ConvRec-R1 enables smaller open-source LLMs to directly produce high-quality recommendations. These results highlight that

432
 433 Table 1: Comparison between ConvRec-R1 and various baselines on the REDDIT-v2 dataset. Here,
 434 R@ k and N@ k stand for Recall@ k and NDCG@ k , respectively.

Method	R@5	R@10	R@15	R@20	N@5	N@10	N@15	N@20
Traditional and Transformer-based CRS								
Redial (Li et al., 2018)	0.0103	0.0228	0.0274	0.0322	0.0073	0.0113	0.0128	0.0143
KBRD (Chen et al., 2019)	0.0444	0.0813	0.1058	0.1223	0.0305	0.0418	0.0490	0.0545
KGSF (Zhou et al., 2020)	0.0579	0.0921	0.1246	0.1433	0.0405	0.0503	0.0599	0.0662
UniCRS (Wang et al., 2022)	0.0722	0.1053	0.1344	0.1494	0.0548	0.0640	0.0726	0.0778
NBCRS (Xie et al., 2024)	0.0801	0.1290	0.1655	0.2019	0.0661	0.0833	0.0954	0.1048
LLM Prompting-Based Methods								
GPT-4o-mini (zero-shot)	0.0949	0.1348	0.1600	0.1687	0.0747	0.0877	0.0950	0.0973
GPT-4o (zero-shot) (He et al., 2023)	0.1106	0.1625	0.1992	0.2147	0.0861	0.1028	0.1136	0.1197
CRAG (Zhu et al., 2025)	0.1146	0.1715	0.2030	0.2212	0.0885	0.1065	0.1164	0.1227
LLM RL Post-Training-Based Methods (off-policy results see Appendix Table 4)								
Most results are significant as standard error are between 0.0020-0.0035 for R@5-20 and 0.0010-0.0025 for N@5-20								
Qwen2.5-0.5B (zero-shot)	0.0021	0.0021	0.0021	0.0021	0.0023	0.0022	0.0021	0.0021
+ SFT	0.0642	0.1027	0.1212	0.1308	0.0502	0.0625	0.0678	0.0704
+ SFT+Vanilla GRPO	0.0834	0.1298	0.1617	0.1803	0.0651	0.0801	0.0895	0.0945
+ SFT+Rank-GRPO (log)	0.0892	0.1353	0.1720	0.1946	0.0701	0.0849	0.0957	0.1017
+ SFT+Rank-GRPO (\exp_{∞})	0.0946	0.1468	0.1813	0.2047	0.0744	0.0915	0.1016	0.1079
Llama-3.2-1B (zero-shot)	0.0187	0.0240	0.0257	0.0263	0.0157	0.0170	0.0175	0.0176
+ SFT	0.0754	0.1148	0.1354	0.1498	0.0595	0.0723	0.0782	0.0819
+ SFT+Vanilla GRPO	0.0979	0.1474	0.1806	0.2037	0.0762	0.0920	0.1026	0.1097
+ SFT+Rank-GRPO (log)	0.1014	0.1527	0.1907	0.2159	0.0792	0.0956	0.1067	0.1134
+ SFT+Rank-GRPO (\exp_{∞})	0.1039	0.1569	0.1937	0.2165	0.0813	0.0985	0.1092	0.1153
Llama-3.2-3B (zero-shot)	0.0574	0.0805	0.0912	0.0961	0.0463	0.0535	0.0566	0.0580
+ SFT	0.0788	0.1191	0.1410	0.1541	0.0615	0.0744	0.0807	0.0842
+ SFT+Vanilla GRPO	0.1034	0.1568	0.1946	0.2186	0.0824	0.0996	0.1106	0.1170
+ SFT+Rank-GRPO (log)	0.1103	0.1638	0.2033	0.2302	0.0862	0.1035	0.1169	0.1239
+ SFT+Rank-GRPO (\exp_{∞})	0.1178	0.1756	0.2150	0.2368	0.0919	0.1107	0.1223	0.1283

461 properly aligned small LLMs can match or even exceed much larger proprietary models in CRS. In
 462 addition, we discuss the comparison between Rank-GRPO and several RL-free post-training base-
 463 lines for LLM-based RSs (Chen et al., 2024; Gao et al., 2025) in Section D.3 of the Appendix.

3.6 ABLATION STUDY

467 In this section, we present an ablation study where we remove the *remap* and *reflect* steps in the
 468 behavior cloning dataset construction, as well as the entire SFT stage. The results are summarized
 469 in Table 2. We observe that SFT plays a crucial role in warming up RL with strong catalog awareness
 470 and a preliminary ability to generate coherent ranked item lists. In particular, removing the *remap*
 471 step significantly harms performance by weakening catalog grounding, while removing the *reflect*
 472 step degrades the quality of the learned ranking, leading to lower Recall/NDCG at larger k . The
 473 full Remap–Reflect–Adjust pipeline followed by SFT and Rank-GRPO thus yields the best overall
 474 performance, confirming that all components contribute meaningfully to the final CRS quality.

4 RELATED WORK

4.1 LLM-BASED CONVERSATIONAL RECOMMENDER SYSTEMS

479 LLM-based conversational recommender systems (CRS) leverage the language understanding and
 480 generation capabilities of LLMs to capture user preferences and deliver recommendations through
 481 dialogue (Zhao et al., 2023; Zhang et al., 2024; Lambert et al., 2024). Early approaches often en-
 482 coded item IDs as special tokens in the model vocabulary, allowing the LLM to generate IDs directly
 483 as recommendations (Hua et al., 2023; Zhu et al., 2024b; Zhang et al., 2025b). More recent work,
 484 however, has highlighted the benefits of representing items in natural language (e.g., titles with at-
 485 tributes or descriptions) and prompting the model to output recommendation lists (He et al., 2023;
 486 Zhang et al., 2025a; Zhu et al., 2025) or rankings (Hou et al., 2024). This natural-language for-

Table 2: Comparison between ConvRec-R1 and various ablation models on the REDDIT-V2 dataset.

Method	R@5	R@10	R@15	R@20	N@5	N@10	N@15	N@20
Qwen2.5-0.5B (SFT)	0.0642	0.1027	0.1212	0.1308	0.0502	0.0625	0.0678	0.0704
– remove remap-reflect step	0.0579	0.0885	0.1111	0.1192	0.0450	0.0548	0.0614	0.0637
– remove reflect step	0.0623	0.0947	0.1190	0.1307	0.0496	0.0600	0.0670	0.0698
Qwen2.5-0.5B (SFT + Rank-GRPO (\exp_{∞}))	0.0946	0.1468	0.1813	0.2047	0.0744	0.0915	0.1016	0.1079
– remove SFT stage (R1-zero)	0.0440	0.0545	0.0584	0.0618	0.0373	0.0405	0.0419	0.0431
Llama-3.2-1B (SFT)	0.0754	0.1148	0.1354	0.1498	0.0595	0.0723	0.0782	0.0819
– remove remap-reflect step	0.0713	0.1085	0.1312	0.1421	0.0574	0.0690	0.0757	0.0786
– remove reflect step	0.0714	0.1102	0.1339	0.1460	0.0576	0.0698	0.0767	0.0800
Llama-3.2-1B (SFT + Rank-GRPO (\exp_{∞}))	0.1039	0.1569	0.1937	0.2165	0.0813	0.0985	0.1092	0.1153
– remove SFT stage (R1-zero)	0.0769	0.1175	0.1426	0.1531	0.0651	0.0771	0.0854	0.0884
Llama-3.2-3B (SFT)	0.0788	0.1191	0.1410	0.1541	0.0615	0.0744	0.0807	0.0842
– remove remap-reflect step	0.0724	0.1187	0.1369	0.1382	0.0611	0.0740	0.0801	0.0809
– remove reflect step	0.0748	0.1236	0.1371	0.1441	0.0619	0.0757	0.0801	0.0818
Llama-3.2-3B (SFT + Rank-GRPO (\exp_{∞}))	0.1178	0.1756	0.2150	0.2368	0.0919	0.1107	0.1223	0.1283
– remove SFT stage (R1-zero)	0.0802	0.1295	0.1639	0.1771	0.0737	0.0898	0.1001	0.1039

mulation of the recommendation task maximally preserves the LLM’s core language generalization and reasoning abilities and enables flexible verbal guidance of the CRS by conditioning on conversational context, attribute constraints, or other objectives such as novelty and diversity (He et al., 2023; Zhang et al., 2024). However, zero-shot generation suffers from catalog unawareness, formatting errors, and a sharp decline in quality toward the end of the recommendation list. While fine-tuning approaches (Luo et al., 2025) or retrieval-augmented generation (RAG) (Zhu et al., 2025) can mitigate these issues, they require large amounts of high-quality data. In contrast, large-scale RL for LLM-based CRS with inexpensive, verifiable rewards remains largely underexplored.

4.2 REINFORCEMENT LEARNING WITH VERIFIABLE REWARD

Reinforcement learning from verifiable rewards (RLVR) has emerged as a central paradigm for aligning LLMs. A core algorithm in this domain is group relative policy optimization (GRPO) (Shao et al., 2024), which estimates advantages by comparing relative rewards across groups of responses. Several extensions, such as DAPO (Yu et al., 2025), Dr. GRPO (Zheng et al., 2025), and GSPO (Liu et al., 2025), have enhanced GRPO through improved length normalization, sample efficiency, and sequence-level stability. Yet, GRPO-style methods remain underexplored for tasks with rank-structured outputs such as recommendation. To our knowledge, only two works, Rec-R1 (Lin et al., 2025) and RecLLM-R1 (Xie et al., 2025), have applied GRPO to recommender systems. Rec-R1 generates item descriptions that are later matched to a catalog to compute rewards, differing from our goal of enabling LLMs to directly generate ranked lists of in-catalog items in natural language. RecLLM-R1 generates lists directly but still applies a sequence-level reward for token-level updates, which misaligns with the structure of ranking tasks and limits performance as reflected in the vanilla GRPO baseline. In contrast, we propose **Rank-GRPO**, which introduces rank-level advantages for precise credit assignment and a rank-level importance ratio based on the geometric mean of item-token probabilities, providing a principled framework for aligning LLMs on rank-structured outputs.

5 CONCLUSION

We introduced **ConvRec-R1**, a two-stage framework for aligning LLM-based conversational recommender systems with reinforcement learning. ConvRec-R1 combines a lightweight distillation pipeline, *Remap-Reflect-Adjust*, with **Rank-GRPO**, a principled extension of GRPO tailored to rank-style outputs, addressing its fundamental misalignment of sequence-level rewards and token-level updates. Empirically, ConvRec-R1 significantly improves the recommendation quality of the base model on the REDDIT-V2 dataset, surpassing GRPO-style baselines and even large zero-shot black-box models in Recall and NDCG. Beyond recommendation, our method shows promise for a broad range of tasks with rank-structured outputs, suggesting new opportunities to adapt RL-based alignment techniques for ranking, retrieval, and other sequential decision-making problems.

540 REFERENCES
541

542 Keqin Bao, Jizhi Zhang, Wenjie Wang, Yang Zhang, Zhengyi Yang, Yanchen Luo, Chong Chen, Fulí
543 Feng, and Qi Tian. A bi-step grounding paradigm for large language models in recommendation
544 systems. *ACM Transactions on Recommender Systems*, 3(4):1–27, 2025.

545 Ralph Allan Bradley and Milton E Terry. Rank analysis of incomplete block designs: I. the method
546 of paired comparisons. *Biometrika*, 39(3/4):324–345, 1952.

547 Qibin Chen, Junyang Lin, Yichang Zhang, Ming Ding, Yukuo Cen, Hongxia Yang, and Jie Tang.
548 Towards knowledge-based recommender dialog system. In *EMNLP*, 2019.

549 Tianqi Chen, Bing Xu, Chiyuan Zhang, and Carlos Guestrin. Training deep nets with sublinear
550 memory cost. *arXiv preprint arXiv:1604.06174*, 2016.

551 Yuxin Chen, Junfei Tan, An Zhang, Zhengyi Yang, Leheng Sheng, Enzhi Zhang, Xiang Wang, and
552 Tat-Seng Chua. On softmax direct preference optimization for recommendation. *NeurIPS*, 37:
553 27463–27489, 2024.

554 Tri Dao. FlashAttention-2: Faster attention with better parallelism and work partitioning. *arXiv
555 preprint arXiv:2307.08691*, 2023.

556 Chongming Gao, Ruijun Chen, Shuai Yuan, Kexin Huang, Yuanqing Yu, and Xiangnan He. SPRec:
557 Self-play to debias LLM-based recommendation. In *WWW*, pp. 5075–5084, 2025.

558 Daya Guo, Dejian Yang, Haowei Zhang, Junxiao Song, Ruoyu Zhang, Runxin Xu, Qihao Zhu,
559 Shirong Ma, Peiyi Wang, Xiao Bi, et al. Deepseek-R1: Incentivizing reasoning capability in
560 LLMs via reinforcement learning. *arXiv preprint arXiv:2501.12948*, 2025.

561 Shirley Anugrah Hayati, Dongyeop Kang, Qingxiaoyang Zhu, Weiyang Shi, and Zhou Yu. Inspired:
562 Toward sociable recommendation dialog systems. In *EMNLP*, pp. 8142–8152, 2020.

563 Zhankui He, Zhouhang Xie, Rahul Jha, Harald Steck, Dawen Liang, Yesu Feng, Bodhisattwa Prasad
564 Majumder, Nathan Kallus, and Julian McAuley. Large language models as zero-shot conversa-
565 tional recommenders. In *CIKM*, pp. 720–730, 2023.

566 Yupeng Hou, Junjie Zhang, Zihan Lin, Hongyu Lu, Ruobing Xie, Julian McAuley, and Wayne Xin
567 Zhao. Large language models are zero-shot rankers for recommender systems. In *ECIR*, pp.
568 364–381. Springer, 2024.

569 Wenyue Hua, Shuyuan Xu, Yingqiang Ge, and Yongfeng Zhang. How to index item IDs for recom-
570 mendation foundation models. In *SIGIR*, pp. 195–204, 2023.

571 Woosuk Kwon, Zhuohan Li, Siyuan Zhuang, Ying Sheng, Lianmin Zheng, Cody Hao Yu, Joseph
572 Gonzalez, Hao Zhang, and Ion Stoica. Efficient memory management for large language model
573 serving with PagedAttention. In *SOSP*, pp. 611–626, 2023.

574 Nathan Lambert, Jacob Morrison, Valentina Pyatkin, Shengyi Huang, Hamish Ivison, Faeze Brah-
575 man, Lester James V Miranda, Alisa Liu, Nouha Dziri, Shane Lyu, et al. Tulu 3: Pushing frontiers
576 in open language model post-training. *arXiv preprint arXiv:2411.15124*, 2024.

577 Patrick Lewis, Ethan Perez, Aleksandra Piktus, Fabio Petroni, Vladimir Karpukhin, Naman Goyal,
578 Heinrich Küttler, Mike Lewis, Wen-tau Yih, Tim Rocktäschel, et al. Retrieval-augmented gener-
579 ation for knowledge-intensive NLP tasks. *NeurIPS*, 33:9459–9474, 2020.

580 Raymond Li, Samira Ebrahimi Kahou, Hannes Schulz, Vincent Michalski, Laurent Charlin, and
581 Chris Pal. Towards deep conversational recommendations. In *NeurIPS*, 2018.

582 Dawen Liang, Rahul G Krishnan, Matthew D Hoffman, and Tony Jebara. Variational autoencoders
583 for collaborative filtering. In *WWW*, pp. 689–698, 2018.

584 Jiacheng Lin, Tian Wang, and Kun Qian. Rec-R1: Bridging generative large language mod-
585 els and user-centric recommendation systems via reinforcement learning. *arXiv preprint
586 arXiv:2503.24289*, 2025.

594 Zichen Liu, Changyu Chen, Wenjun Li, Penghui Qi, Tianyu Pang, Chao Du, Wee Sun Lee,
 595 and Min Lin. Understanding R1-Zero-like training: A critical perspective. *arXiv preprint*
 596 *arXiv:2503.20783*, 2025.

597 Sichun Luo, Bowei He, Haohan Zhao, Wei Shao, Yanlin Qi, Yinya Huang, Aojun Zhou, Yuxuan
 598 Yao, Zongpeng Li, Yuanzhang Xiao, et al. RecRanker: Instruction tuning large language model
 599 as ranker for top-k recommendation. *ACM TOIS*, 43(5):1–31, 2025.

600 Long Ouyang, Jeffrey Wu, Xu Jiang, Diogo Almeida, Carroll Wainwright, Pamela Mishkin, Chong
 601 Zhang, Sandhini Agarwal, Katarina Slama, Alex Ray, et al. Training language models to follow
 602 instructions with human feedback. *NeurIPS*, 35:27730–27744, 2022.

603 Rafael Rafailov, Archit Sharma, Eric Mitchell, Christopher D Manning, Stefano Ermon, and Chelsea
 604 Finn. Direct preference optimization: Your language model is secretly a reward model. *NeurIPS*,
 605 36:53728–53741, 2023.

606 Samyam Rajbhandari, Jeff Rasley, Olatunji Ruwase, and Yuxiong He. Zero: Memory optimizations
 607 toward training trillion parameter models. In *Supercomputing Conference*, pp. 1–16, 2020.

608 Nils Reimers and Iryna Gurevych. Sentence-BERT: Sentence embeddings using siamese BERT-
 609 networks. In *EMNLP*, pp. 3982–3992, 2019.

610 John Schulman, Filip Wolski, Prafulla Dhariwal, Alec Radford, and Oleg Klimov. Proximal policy
 611 optimization algorithms. *arXiv preprint arXiv:1707.06347*, 2017.

612 Zhihong Shao, Peiyi Wang, Qihao Zhu, Runxin Xu, Junxiao Song, Xiao Bi, Haowei Zhang,
 613 Mingchuan Zhang, YK Li, et al. Deepseekmath: Pushing the limits of mathematical reasoning in
 614 open language models. *arXiv preprint arXiv:2402.03300*, 2024.

615 Richard S Sutton, David McAllester, Satinder Singh, and Yishay Mansour. Policy gradient methods
 616 for reinforcement learning with function approximation. *NeurIPS*, 12, 1999.

617 Xiaolei Wang, Kun Zhou, Ji-Rong Wen, and Wayne Xin Zhao. Towards unified conversational
 618 recommender systems via knowledge-enhanced prompt learning. In *KDD*, pp. 1929–1937, 2022.

619 Zhepei Wei, Wenlin Yao, Yao Liu, Weizhi Zhang, Qin Lu, Liang Qiu, Changlong Yu, Puyang Xu,
 620 Chao Zhang, Bing Yin, et al. Webagent-r1: Training web agents via end-to-end multi-turn rein-
 621 forcement learning. *arXiv preprint arXiv:2505.16421*, 2025.

622 Junda Wu, Rohan Surana, Zhouhang Xie, Yiran Shen, Yu Xia, Tong Yu, Ryan A Rossi, Prithviraj
 623 Ammanabrolu, and Julian McAuley. In-context ranking preference optimization. *COLM*, 2025.

624 Yu Xie, Xingkai Ren, Ying Qi, Yao Hu, and Lianlei Shan. RecLLM-R1: A two-stage training
 625 paradigm with reinforcement learning and chain-of-thought v1. *arXiv preprint arXiv:2506.19235*,
 626 2025.

627 Zhouhang Xie, Junda Wu, Hyunsik Jeon, Zhankui He, Harald Steck, Rahul Jha, Dawen Liang,
 628 Nathan Kallus, and Julian McAuley. Neighborhood-based collaborative filtering for conversa-
 629 tional recommendation. In *RecSys*, pp. 1045–1050, 2024.

630 An Yang, Anfeng Li, Baosong Yang, Beichen Zhang, Binyuan Hui, Bo Zheng, Bowen Yu,
 631 Chang Gao, Chengan Huang, Chenxu Lv, et al. Qwen3 technical report. *arXiv preprint*
 632 *arXiv:2505.09388*, 2025.

633 Qiying Yu, Zheng Zhang, Ruofei Zhu, Yufeng Yuan, Xiaochen Zuo, Yu Yue, Weinan Dai, Tiantian
 634 Fan, Gaohong Liu, Lingjun Liu, et al. DAPO: An open-source LLM reinforcement learning
 635 system at scale. *arXiv preprint arXiv:2503.14476*, 2025.

636 An Zhang, Yuxin Chen, Leheng Sheng, Xiang Wang, and Tat-Seng Chua. On generative agents in
 637 recommendation. In *SIGIR*, pp. 1807–1817, 2024.

638 Junjie Zhang, Ruobing Xie, Yupeng Hou, Xin Zhao, Leyu Lin, and Ji-Rong Wen. Recommendation
 639 as instruction following: A large language model empowered recommendation approach. *ACM*
 640 *TOIS*, 43(5):1–37, 2025a.

648 Yang Zhang, Fuli Feng, Jizhi Zhang, Keqin Bao, Qifan Wang, and Xiangnan He. CoLLM: Integrat-
 649 ing collaborative embeddings into large language models for recommendation. *IEEE Transactions*
 650 *on Knowledge and Data Engineering*, 2025b.

651 Wayne Xin Zhao, Kun Zhou, Junyi Li, Tianyi Tang, Xiaolei Wang, Yupeng Hou, Yingqian Min,
 652 Beichen Zhang, Junjie Zhang, Zican Dong, et al. A survey of large language models. *arXiv*
 653 *preprint arXiv:2303.18223*, 1(2), 2023.

654 Chujie Zheng, Shixuan Liu, Mingze Li, Xiong-Hui Chen, Bowen Yu, Chang Gao, Kai Dang,
 655 Yuqiong Liu, Rui Men, An Yang, et al. Group sequence policy optimization. *arXiv preprint*
 656 *arXiv:2507.18071*, 2025.

657 Kun Zhou, Wayne Xin Zhao, Shuqing Bian, Yuanhang Zhou, Ji-Rong Wen, and Jingsong Yu. Im-
 658 proving conversational recommender systems via knowledge graph based semantic fusion. In
 659 *KDD*, pp. 1006–1014, 2020.

660 Qihao Zhu, Daya Guo, Zhihong Shao, Dejian Yang, Peiyi Wang, Runxin Xu, Y Wu, Yukun Li,
 661 Huazuo Gao, Shirong Ma, et al. Deepseek-coder-v2: Breaking the barrier of closed-source models
 662 in code intelligence. *arXiv preprint arXiv:2406.11931*, 2024a.

663 Yaochen Zhu, Liang Wu, Qi Guo, Liangjie Hong, and Jundong Li. Collaborative large language
 664 model for recommender systems. In *WWW 2024*, pp. 3162–3172, 2024b.

665 Yaochen Zhu, Chao Wan, Harald Steck, Dawen Liang, Yesu Feng, Nathan Kallus, and Jundong Li.
 666 Collaborative retrieval for large language model-based conversational recommender systems. In
 667 *WWW*, pp. 3323–3334, 2025.

668
 669
 670
 671
 672
 673
 674
 675
 676
 677
 678
 679
 680
 681
 682
 683
 684
 685
 686
 687
 688
 689
 690
 691
 692
 693
 694
 695
 696
 697
 698
 699
 700
 701

APPENDIX

A DETAILS FOR THE REMAP-REFLECT-ADJUST PIPELINE

This section provides the detail for the **Remap-Reflect-Adjust** pipeline used to generate the catalog-grounded behavior cloning dataset for the supervised fine-tuning (SFT) stage of ConvRecR1 (see Section 2.2). We note that the following pipeline is specifically designed for the movie recommendation task, but the generalization to other items generally follows a similar procedure.

A.1 STEP 1. REMAP

The **remap** step aims to ground the raw recommendations $y_{i,\text{raw}}^{\text{SFT}}$ in the teacher LLM’s recommendation space \mathcal{C}_Θ , into a score vector $s_{\text{remap}} \in \mathbb{R}^{|\mathcal{C}|}$ in the target catalog space \mathcal{C} . The process involves three components: item metadata generation, similarity calculation, and score aggregation.

A.1.1 METADATA GENERATION

To facilitate semantic similarity-based remapping, we first generate consistent and comprehensive metadata for every item in both \mathcal{C}_Θ and \mathcal{C} . Based on whether the teacher LLM Θ has the knowledge of the item and whether the item is in the catalog, we have the following three cases:

- (i) **For in-catalog items known to teacher LLM Θ** , we use a zero-shot prompt to generate a summary including keywords and a plot description. This ensures a consistent style and broad coverage of aspects that facilitate high-quality item-item similarity calculation.
- (ii) **For out-of-catalog (OOC) or hallucinated items**. Since these items are recommended by the LLM, it can still generate plausible metadata crucial for mapping them back to the catalog.
- (iii) **For in-catalog items unknown to the LLM** (e.g., niche or recent items), we employ retrieval augmented generation (RAG) (Lewis et al., 2020) and in-context learning (ICL). We retrieve external information about the item via Google Search API on Wikipedia, IMDb, and Rotten Tomatoes and provide it to the LLM along with few-shot examples to guide the generation.

The prompts we are using to generate the metadata for known/unknown items are as follows.

Prompt to Generate Metadata for Items Known to the Teacher LLM Θ

```
Summarize the metadata for the movie movie_name (release year)
based on the information in the format of:
Movie_Name (Release_Year)
Keywords:
<comma-separated keywords>
Plots:
<one-paragraph plot summary>

You should separate the keywords with commas without numbering.
The plot should be one paragraph.
```

Prompt to Generate Metadata for Items Unknown to the Teacher LLM Θ with RAG and ICL

```
Summarize the metadata for the movie movie_name (release year)
based on the information in the format of:
Movie_Name (Release_Year)
Keywords:
<comma-separated keywords>
Plots:
<one-paragraph plot summary>

You should separate the keywords with commas without numbering.
The plot should be one paragraph.

Here are the information related to the target movie: {movie_info}
Here are some examples for the generated metadata for different movies: {examples}
```

756 Here we provide some examples of the generated metadata as follows:
 757

758 **Examples for the Generated Metadata in the Remap Step**

759 **Case (i). In-catalog items known to teacher LLM**
 760 **Stranger Things (2016)**

761 **Keywords:** supernatural, mystery, 1980s, parallel universe, friendship,
 762 government conspiracy, small town, telekinesis, missing child, monster
 763 **Plots:** In the small town of Hawkins, Indiana, the sudden disappearance of a
 764 young boy named Will Byers sets off a chain of events that unravels a series of
 765 supernatural mysteries. As his friends and family search for him, they encounter
 766 a mysterious girl with telekinetic powers who may hold the key to finding Will.
 767 Meanwhile, a secretive government agency conducts experiments that open a portal
 768 to a parallel universe, unleashing terrifying creatures into the town...

769 **Case (ii). Out-of-catalog (OOC) or hallucinated items**
 770 **The Divergent Series (2014) (a series but not a movie)**

771 **Keywords:** dystopian, factions, rebellion, identity, society, future, action,
 772 adventure, science fiction, young adult, survival, government, control, freedom
 773 **Plots:** In a future society divided into five distinct factions based on human
 774 virtues, everyone must choose where they belong. Tris Prior discovers she
 775 is Divergent, meaning she doesn't fit into any one group. As she uncovers a
 776 conspiracy to eliminate all Divergents, Tris must rely on her unique abilities
 777 to survive and protect those she loves. With the help of the mysterious Four,
 778 she embarks on a journey of self-discovery and rebellion against the oppressive
 779 system, challenging the status quo and fighting for freedom.

780 **Case (iii). In-catalog items UNKNOWN to teacher LLM**
 781 **La strada verso casa (2011)**

782 **Keywords:** drama, pain, death, life, Michelangelo, Antonio, Giulia, Italy, subtle
 783 pressures, intertwine, healing
 784 **Plots:** "La strada verso casa" tells the poignant story of Michelangelo, Antonio,
 785 and Giulia, three individuals whose lives are abruptly disrupted by pain and
 786 death. As they face their personal struggles, they find solace and strength in
 787 each other, subtly influencing one another's paths. Through their intertwined
 788 journeys, they navigate the complexities of grief and healing, ultimately
 789 discovering a renewed sense of life and purpose. Set against the backdrop of
 790 Italy, the film explores themes of connection, resilience, and the transformative
 791 power of human relationships.

792 **A.1.2 SIMILARITY AND SCORE CALCULATION**

793 With the generated metadata for items in \mathcal{C}_Θ and \mathcal{C} in place, we compute two types of similarities:

794 **(i) Item-Item Similarity ($S_{\text{item-item}}$):** We calculate the content-based semantic similarity be-
 795 between every item in the teacher's space \mathcal{C}_Θ and every item in the target catalog \mathcal{C} . The gen-
 796 erated metadata are embedded using a pre-trained sentence-transformer model (Reimers &
 797 Gurevych, 2019) (we use NovaSearch/stella_en_400M_v5 in this paper). The cosine similarity
 798 between these embeddings forms the item-item similarity matrix $S_{\text{item-item}} \in \mathbb{R}^{|\mathcal{C}_\Theta| \times |\mathcal{C}|}$.
 799 **(ii) Conversation-Item Similarity (s_{context}):** To further enhance the contextual relevance, we
 800 compute the similarity between the conversation x_i^{SFT} and each item in the catalog \mathcal{C} . We
 801 embed x_i^{SFT} with the same Stella model and its cosine similarity with each catalog item's
 802 metadata embedding is calculated, resulting in a context vector $s_{\text{context}} \in \mathbb{R}^{|\mathcal{C}|}$.

803 The final remapped scores are calculated by aggregating the signals from the teacher's raw recom-
 804 mendations $y_{i,\text{raw}}^{\text{SFT}}$, and $S_{\text{item-item}}$, s_{context} as follows:

$$s_{\text{remap}} = \mathbf{p} \cdot (S_{\text{item-item}} + I_{\text{ic}}) + \lambda \cdot s_{\text{context}}, \quad (10)$$

805 where $\mathbf{p} \in \mathbb{R}^{|\mathcal{C}_\Theta|}$ is a sparse vector representing the **positional scores** of items in the teacher's
 806 raw recommendation list. The score for an item at rank k is heuristically set to $1/\sqrt{k}$, and 0 for
 807 items not present, $I_{\text{ic}} \in \{0, 1\}^{|\mathcal{C}_\Theta| \times |\mathcal{C}|}$ is a sparse indicator mapping matrix with $I_{\text{ic}}[u, v] = 1$
 808 iff the u -th item in \mathcal{C}_Θ equals the v -th catalog item, which directly transfer the positional scores
 809 of any recommended items that are already in the catalog, λ is a hyperparameter that weights the
 810 importance of the conversation-item similarity for the remapping. In the paper, we set $\lambda = 1$.

810 A.2 STEP 2. REFLECT
811

812 The **reflect** step adjusts the ranking of the top candidates from the *remap* stage by leveraging the
813 teacher LLM’s judgment on the contextual relevancy w.r.t the conversation x_i^{SFT} . While the remapping
814 step grounds the raw recommendations from the teacher $y_{i,\text{raw}}^{\text{SFT}}$ to the catalog space as s_{remap} , the
815 ranking may not be perfectly aligned with the nuances of the user’s conversational context as they
816 are conducted based on embedding models, which are known to be relatively insufficient to cap-
817 ture multiple aspects and subtle preferences behind the lines that are crucial for recommendations.
818 Therefore, we leverage LLM-as-a-judge to rate the top- $N_r > N$ items (e.g., top 100) from s_{remap}
819 based on their suitability for the conversation. We use the following prompt template:

820 **Prompt for LLM-as-a-Judge in the *reflect* step**
821
822 Pretend you are a movie recommender system. I will give you a
823 conversation between a user and you (a recommender system) as well
824 as some movie candidates from our movie database.
825
826 You need to rate each retrieved movie as recommendations into five
827 levels based on the conversation:
828 2 (great), 1 (good), 0 (normal), -1 (not good), -2 (bad).
829
830 Here is the conversation: {context}
831 Here are the movie candidates: {rec_titles}.
832
833 You need to reply with the rating of each movie in a line, in the
834 form of movie_name (release_year) ####rating

835 The numerical ratings from the LLM form a sparse reflection vector $r_{\text{reflect}} \in \mathbb{R}^{|C|}$. This vector is
836 then scaled by a hyperparameter γ and added to the remapped scores to produce the reflected scores:
837

$$s_{\text{reflect}} = s_{\text{remap}} + \gamma \cdot r_{\text{reflect}}. \quad (11)$$

838 This step helps to elevate contextually more relevant items to higher ranks, and therefore further
839 improves the quality of the exemplar ranking demonstration data. In this paper, we choose five-scale
840 reflection scores from $[-2, 2]$ representing bad to great and therefore γ is set to 0.5 to normalize the
841 reflection scores to $[-1, 1]$, which has a similar scale as s_{remap} .

842 A.3 ADJUST
843

844 Finally, the **adjust** step is a valuable final stage that corrects for residual popularity biases that may
845 be inherited from the teacher model or the remapping process due to its unawareness of the current
846 trend. Specifically, we align the score distribution with the empirical distribution observed in the
847 groundtruth training data (i.e., items with positive user feedback). This is framed as a residual
848 learning problem. We learn an item-specific multiplicative bias vector $w \in \mathbb{R}^{|C|}$ and an additive
849 bias vector $b \in \mathbb{R}^{|C|}$ to fine-tune the scores. The final, adjusted scores are computed as:

$$s_{\text{final}} = w \odot s_{\text{reflect}} + b, \quad (12)$$

850 where \odot denotes the element-wise product. The vectors w and b are optimized by maximizing the
851 multinomial log-likelihood of observing the groundtruth positive items from the training data $\mathcal{D}_{\text{train}}$
852 (Liang et al., 2018). If we denote the groundtruth items for a conversation as a multi-hot vector y_i^{gt} ,
853 the optimization objective can be formulated as:

$$\mathcal{L}_{\text{adjust}} = - \sum_{i \in \mathcal{D}_{\text{train}}} \sum_{j: y_{i,j}^{\text{gt}} = 1} \log \frac{\exp((w \odot s_{\text{reflect},i} + b)_j)}{\sum_{k \in \mathcal{C}} \exp((w \odot s_{\text{reflect},i} + b)_k)} + \lambda_w \|w - \mathbf{1}\|_2^2 + \lambda_b \|b\|_2^2, \quad (13)$$

854 where λ_w and λ_b are hyperparameters for weight decay and are set to 0.01. After this final adjust-
855 ment step, for each training conversation x_i^{SFT} , the top- N items from the catalog are selected based
856 on their scores in s_{final} to form the final, high-quality demonstration list y_i^{SFT} used in the SFT stage.
857

858 A.4 EXAMPLE OF DEMONSTRATION GENERATED BY REMAP-REFLECT-ADJUST PIPELINE
859

860 In this section, we present an example from the constructed behavior cloning dataset \mathcal{D}_{SFT} for
861 ConvRec-R1, along with a qualitative ablation study of the *Remap-Reflect-Adjust* pipeline. The
862

example illustrates given a conversation x_i^{SFT} , how the the teacher's zero-shot recommendations and the intermediate results evolve across each stage of the pipeline. To facilitate future research on LLM-based CRS, we also release the behavior cloning dataset, together with the accompanying code and trained models, at <https://anonymous.4open.science/r/ConvRec-R1-5615/>.

Exemplar Demonstrations from the Remap-Reflect-Adjust Pipeline

(i) Conversation x_i^{SFT} :

User: any good ocean sailing movies like master and commander?. I would prefer more of the old days and not something with submarines/ww2 but I did like hunt for red october a lot. Just looking for something like master and commander. It doesn't necessarily have to be military; can be pirates too. I know of the obvious stuff like pirates of caribbean movies, that new netflix animated ocean movie with jared harris/karl urban, waterworld (lmao), ect.
i think I made this topic before and someone suggested horatio hornblower. I liked the show of the few episodes I watched but had to watch it on youtube and didn't like the quality and I don't think it had subtitles, which is almost a must for me. Appreciate any suggestions.

(ii) Groundtruth y_i^{gt} :

1492: Conquest of Paradise (1992)

(iii) Outputs from the Remap-Reflect-Adjust Pipeline:

Rk.	Zero-Shot $y_{i,\text{raw}}^{\text{SFT}}$ (OOC titles in red)	Step 1. Remap
1	Mutiny on the Bounty (1935)	The Bounty (1984)
2	The Bounty (1984)	Captain Blood (1935)
3	Captain Blood (1935)	The Sea Hawk (1940)
4	The Sea Hawk (1940)	Treasure Island (1950)
5	Treasure Island (1950)	The Crimson Pirate (1952)
6	Moby Dick (1956)	The Spanish Main (1945)
7	The Buccaneer (1958)	Cutthroat Island (1995)
8	Billy Budd (1962)	The Adventures of Robin Hood (1938)
9	Swashbuckler (1976)	The Vikings (1958)
10	The Black Swan (1942)	Master and Commander (2003)
11	The Crimson Pirate (1952)	Run Silent Run Deep (1958)
12	Damn the Defiant! (1962)	Das Boot (1981)
13	The Long Ships (1964)	Black Sails (2014)
14	The Black Pirate (1926)	Captain Phillips (2013)
15	Cutthroat Island (1995)	The Caine Mutiny (1954)
16	The Adventures of Robin Hood (1938)	Greyhound (2020)
17	The Vikings (1958)	Captains Courageous (1937)
18	The Sea Wolf (1941)	20,000 Leagues Under the Sea (1954)
19	The Spanish Main (1945)	In the Heart of the Sea (2015)
20	Against All Flags (1952)	The Wreck of the Mary Deare (1959)
Rk.	Step 2. Reflect (vs. Remap)	Step 3. Adjust y_i^{SFT} (with popularity)
1	The Bounty (1984)	The Bounty (1984) 56
2	Captain Blood (1935)	Captain Blood (1935) 31
3	The Sea Hawk (1940)	Master and Commander (2003) 262 ▲2
4	Treasure Island (1950)	Das Boot (1981) 523 ▲3
5	Master and Commander (2003) ▲5	The Sea Hawk (1940) 17 ▼2
6	The Crimson Pirate (1952) ▼1	Treasure Island (1950) 27 ▼2
7	Das Boot (1981) ▲5	Cutthroat Island (1995) 66
8	The Spanish Main (1945) ▼2	The Adventures of Robin Hood (1938) 120
9	Cutthroat Island (1995) ▼2	The Crimson Pirate (1952) 7 ▼1
10	The Adventures of Robin Hood (1938) ▼2	The Vikings (1958) 24
11	The Vikings (1958) ▼2	Run Silent Run Deep (1958) 27
12	Run Silent Run Deep (1958) ▼1	The Spanish Main (1945) 3
13	Black Sails (2014)	Black Sails (2014) 103
14	Captain Phillips (2013)	Captain Phillips (2013) 183
15	The Caine Mutiny (1954)	The Caine Mutiny (1954) 59
16	Greyhound (2020)	Greyhound (2020) 78
17	Captains Courageous (1937)	Captains Courageous (1937) 25
18	20,000 Leagues Under the Sea (1954)	20,000 Leagues Under the Sea (1954) 98
19	In the Heart of the Sea (2015)	In the Heart of the Sea (2015) 71
20	The Wreck of the Mary Deare (1959)	The Wreck of the Mary Deare (1959) 2

918 B GRADIENT ANALYSIS FOR GRPO, GSPO AND RANK-GRPO

920 In this section, we provide the full policy gradient derivations for GRPO (Shao et al., 2024), GSPO
 921 (Zheng et al., 2025), and our proposed Rank-GRPO. The clipping term from the PPO-style objective
 922 is omitted for brevity. All derivations leverage the log-derivative trick (Sutton et al., 1999), which
 923 states that for a function $f(\theta)$, its gradient can be expressed as $\nabla_{\theta} f(\theta) = f(\theta) \nabla_{\theta} \log f(\theta)$. This
 924 allows us to rewrite the gradient of the objective in a form suitable for sampling-based estimation.

925 **(i) GRPO.** The gradient of the GRPO objective is derived with the following steps. We start by
 926 bringing the gradient operator inside the expectation based on the interchangeability of integration
 927 and differentiation. Then we apply the gradient to the terms dependent on θ (which is only the
 928 importance ratio $w_{i,t}(\theta)$), and then use the log-derivative trick as follows:

$$\begin{aligned}
 930 \nabla_{\theta} \mathcal{J}_{\text{GRPO}}(\theta) &= \nabla_{\theta} \mathbb{E}_{\pi_{\theta_{\text{old}}}} \left[\frac{1}{G} \sum_{i=1}^G \frac{1}{|y_i|} \sum_{t=1}^{|y_i|} w_{i,t}(\theta) \hat{A}_{i,t} \right] = \mathbb{E}_{\pi_{\theta_{\text{old}}}} \left[\frac{1}{G} \sum_{i=1}^G \frac{1}{|y_i|} \sum_{t=1}^{|y_i|} \hat{A}_{i,t} \nabla_{\theta} w_{i,t}(\theta) \right] \\
 931 &= \mathbb{E}_{\pi_{\theta_{\text{old}}}} \left[\frac{1}{G} \sum_{i=1}^G \frac{1}{|y_i|} \sum_{t=1}^{|y_i|} \hat{A}_{i,t} w_{i,t}(\theta) \nabla_{\theta} \log w_{i,t}(\theta) \right] \quad (\text{Log-derivative trick}) \\
 932 &= \mathbb{E}_{\pi_{\theta_{\text{old}}}} \left[\frac{1}{G} \sum_{i=1}^G \frac{1}{|y_i|} \sum_{t=1}^{|y_i|} w_{i,t}(\theta) \hat{A}_{i,t} \nabla_{\theta} \log \pi_{\theta}(y_{i,t}|x, y_{i,<t}) \right] \\
 933 &\propto \mathbb{E}_{\pi_{\theta_{\text{old}}}} \left[\sum_{i=1}^G \frac{1}{|y_i|} \sum_{t=1}^{|y_i|} \underbrace{w_{i,t}(\theta)}_{\text{token (t)-level importance ratio}} \cdot \underbrace{\hat{A}_{i,t}}_{\text{sequence (i)-level advantage}} \cdot \underbrace{\nabla_{\theta} \log \pi_{\theta}(y_{i,t}|x, y_{i,<t})}_{\text{token (t)-level gradient of log-likelihood}} \right]. \tag{14}
 \end{aligned}$$

943 From Eq. (14), we see that GRPO updates the token-level policy using sequence-level rewards. This
 944 introduces two sources of misalignment: **(i)** the importance ratio is defined at the token level, while
 945 the reward is defined at the sequence level, conflicting with the principle of importance sampling
 946 (Zheng et al., 2025); and **(ii)** the reward signal is too coarse for ranking tasks, whereas token-level
 947 updates are overly fine-grained. Together, these mismatches make the vanilla GRPO algorithm
 948 fundamentally ill-suited for reinforcement learning on rank-structured outputs.

949 **(ii) GSPO.** Different from GRPO that combines sequence-level rewards with token-level updates,
 950 group sequence policy optimization (GSPO) defines both the reward and the importance ratio at the
 951 sequence level. Its derivation largely follows Eq. (14) as follows:

$$\begin{aligned}
 953 \nabla_{\theta} \mathcal{J}_{\text{GSPO}}(\theta) &= \nabla_{\theta} \mathbb{E}_{\pi_{\theta_{\text{old}}}} \left[\frac{1}{G} \sum_{i=1}^G s_i(\theta) \hat{A}_i \right] = \mathbb{E}_{\pi_{\theta_{\text{old}}}} \left[\frac{1}{G} \sum_{i=1}^G \hat{A}_i \nabla_{\theta} s_i(\theta) \right] \\
 954 &= \mathbb{E}_{\pi_{\theta_{\text{old}}}} \left[\frac{1}{G} \sum_{i=1}^G s_i(\theta) \hat{A}_i \nabla_{\theta} \log s_i(\theta) \right] \quad (\text{Log-derivative trick}) \\
 955 &= \mathbb{E}_{\pi_{\theta_{\text{old}}}} \left[\frac{1}{G} \sum_{i=1}^G s_i(\theta) \hat{A}_i \left(\frac{1}{|y_i|} \sum_{t=1}^{|y_i|} \nabla_{\theta} \log \pi_{\theta}(y_{i,t}|x, y_{i,<t}) \right) \right] \\
 956 &\propto \mathbb{E}_{\pi_{\theta_{\text{old}}}} \left[\sum_{i=1}^G \underbrace{s_i(\theta)}_{\text{sequence (i)-level importance ratio}} \cdot \underbrace{\hat{A}_i}_{\text{sequence (i)-level advantage}} \cdot \underbrace{\frac{1}{|y_i|} \sum_{t=1}^{|y_i|} \nabla_{\theta} \log \pi_{\theta}(y_{i,t}|x, y_{i,<t})}_{\text{sequence (i)-level gradient of log-likelihood}} \right], \tag{15}
 \end{aligned}$$

957 where $s_i(\theta) = \left(\frac{\pi_{\theta}(y_i|x)}{\pi_{\theta_{\text{old}}}(y_i|x)} \right)^{1/|y_i|}$ is the length-normalized sequence importance ratio. From
 958 Eq. (15), we observe that GSPO aligns the importance ratio with sequence-level rewards, which
 959 has been shown to stabilize training in mixture-of-experts models such as Qwen3 series (Yang et al.,
 960 2025) where different experts may be activated between the roll-out and current policies. However,
 961 both the reward and importance ratio remain too coarse for rank-structured tasks, where each rank
 962 should naturally serve as the action unit rather than the entire sequence.

972 **(iii) Rank-GRPO.** Finally, for the Rank-GRPO proposed in this paper, the objective, advantage, and
 973 importance ratio are all defined at the rank level, where the gradient can be derived as follows:
 974

$$\begin{aligned}
 975 \nabla_{\theta} \mathcal{J}_{\text{Rank-GRPO}}(\theta) &= \nabla_{\theta} \mathbb{E}_{\pi_{\theta_{\text{old}}}} \left[\frac{1}{GN} \sum_{i=1}^G \sum_{k=1}^N w_{i,k}(\theta) \hat{A}_{i,k} \right] = \mathbb{E}_{\pi_{\theta_{\text{old}}}} \left[\frac{1}{GN} \sum_{i=1}^G \sum_{k=1}^N \hat{A}_{i,k} \nabla_{\theta} w_{i,k}(\theta) \right] \\
 976 &= \mathbb{E}_{\pi_{\theta_{\text{old}}}} \left[\frac{1}{GN} \sum_{i=1}^G \sum_{k=1}^N w_{i,k}(\theta) \hat{A}_{i,k} \nabla_{\theta} \log w_{i,k}(\theta) \right] \quad (\text{Log-derivative trick}) \\
 977 &= \mathbb{E}_{\pi_{\theta_{\text{old}}}} \left[\frac{1}{GN} \sum_{i=1}^G \sum_{k=1}^N w_{i,k}(\theta) \hat{A}_{i,k} \nabla_{\theta} \log \bar{\pi}_{\theta}(y_i^{(k)} | x) \right] \\
 978 &\propto \mathbb{E}_{\pi_{\theta_{\text{old}}}} \left[\frac{1}{N} \sum_{i=1}^G \sum_{k=1}^N w_{i,k}(\theta) \hat{A}_{i,k} \nabla_{\theta} \log \bar{\pi}_{\theta}(y_i^{(k)} | x) \right] \\
 979 &= \mathbb{E}_{\pi_{\theta_{\text{old}}}} \left[\sum_{i=1}^G \sum_{k=1}^N \underbrace{w_{i,k}(\theta)}_{\text{rank (k)-level importance ratio}} \cdot \underbrace{\hat{A}_{i,k}}_{\text{rank (k)-level advantage}} \cdot \underbrace{\frac{1}{N|y_i^{(k)}|} \sum_{t=1}^{|y_i^{(k)}|} \nabla_{\theta} \log \pi_{\theta}(y_{i,k,t} | x, y_{i,k,<t})}_{\text{rank (k)-level gradient of log-likelihood}} \right]. \tag{16}
 \end{aligned}$$

992 Here, $w_{i,k}(\theta) = \frac{\bar{\pi}_{\theta}(y_i^{(k)} | x)}{\bar{\pi}_{\theta_{\text{old}}}(y_i^{(k)} | x)}$ denotes the rank-level importance ratio, and $\bar{\pi}_{\theta}$ is the length-normalized
 993 item probability, computed as the geometric mean of its token probabilities. From Eq. (16), we see
 994 that Rank-GRPO fundamentally resolves the shortcomings of GRPO and GSPO for rank-structured
 995 outputs. By treating each rank as the action unit, it provides a more natural granularity for both
 996 credit assignment and importance weighting, leading to more stable and task-aligned optimization.
 997

998 C IMPLEMENTATION DETAILS

1000 **(i) Training Setup.** All models are trained on a single node via full-parameter fine-tuning. The
 1001 smaller models (Qwen2.5-0.5B-Instruct, Llama-3.2-1B-Instruct) were trained on a single node with
 1002 four NVIDIA H100 GPUs, each with 80GB of memory. The larger Llama-3.2-3B-Instruct model
 1003 was trained on four NVIDIA H200 GPUs, each with 141GB of memory.

1004 **(ii) Optimization and Efficiency.** To optimize GPU utilization and training speed, we adopt several
 1005 standard techniques. We use *DeepSpeed* (Rajbhandari et al., 2020) with the *ZeRO-3* offload strategy
 1006 for distributed training. We also enable *gradient checkpointing* (Chen et al., 2016), *FlashAttention2*
 1007 (Dao, 2023), and *bf16* mixed-precision training to improve computational efficiency. The effective
 1008 batch size for most experiments is set to 384, which is calculated as follows:
 1009

$$\text{batch_size} = \# \text{GPUs} \times \text{Per_GPU_batch_size} \times \text{Gradient_Accumulation_Steps} \tag{17}$$

1010 **(iii) Hyperparameters for the SFT stage.** For the SFT stage, we use a learning rate of 5×10^{-5}
 1011 with a cosine learning rate scheduler that includes a 5% warm-up period.
 1012

1013 **(iv) Hyperparameters for the RL stage.** For the RL stage, we first tune the learning rate and KL
 1014 weights for the GRPO baseline and apply the same hyperparameters to Rank-GRPO to ensure a fair
 1015 comparison that slightly favors the baseline. For the *on-policy experiments* (Section 3.4), we use a
 1016 learning rate of 1×10^{-6} for the 0.5B model, and 1×10^{-6} with a decay to 1×10^{-7} for the 1B and
 1017 3B models to prevent collapse due to larger size. For the *off-policy experiments* (Section 3.4, with
 1018 $\mu = 2$), we keep the same learning rate for the 0.5B model but halve it to 5×10^{-7} with a decay
 1019 to 5×10^{-8} for the 3B models to account for the instability of importance weighting. In addition,
 1020 we found that training is comparatively less stable for the 1B model (which we attribute to the base
 1021 model itself as training for both 0.5B and 3B backbones are stable), so we adopt a finer-grained
 1022 schedule $5 \times 10^{-7} \rightarrow 2.5 \times 10^{-7} \rightarrow 1 \times 10^{-7} \rightarrow 5 \times 10^{-8}$ to prevent divergence. The KL
 1023 coefficient is set to 0.001. The clip range ϵ_{low} and ϵ_{high} is set to 0.2 and 0.26 for GRPO and 0.06
 1024 and 0.08 for Rank-GRPO to ensure a similar expected clipping range after applying the rank-wise
 1025 geometric mean and effective rank probabilities. The clip range for GSPO is set to $3e-4$ and $4e-4$ as
 recommended by the paper (Zheng et al., 2025). For Rank-GRPO, both ϵ_o and ϵ_u are set to -0.1 .

1026 (v) **Inference and Generation.** For efficient LLM rollouts during the RL stage, we use **vLLM**
 1027 (Kwon et al., 2023) with a tensor parallel size of 2 for the 0.5B and 1B models and 4 for the
 1028 3B model. We set the GPU memory utilization ratio to 0.5. All rollouts are generated with both
 1029 temperature and top- p (for nucleus sampling) set to 1.0, respectively.
 1030

1031 D ADDITIONAL EXPERIMENTAL DETAILS AND RESULTS

1032 D.1 PROMPT USED TO GENERATE RECOMMENDATIONS

1035 Following He et al. (2023) and Zhu et al. (2025), we fix the number of required recommendations
 1036 to $N = 20$ and use a consistent prompt across all experiments to elicit item recommendation lists
 1037 from the LLMs. The prompt explicitly instructs the model to output standardized English movie
 1038 titles with release years in a line-by-line format, ensuring uniformity and facilitating evaluation.
 1039

1040 **Prompt to Generate Recommendations**

1041 Pretend you are a movie recommender system.
 1042 I will give you a conversation between a user and you (a recommender system).
 1043 Based on the conversation, you need to reply with 20 recommendations.
 1044
 1045 List the standardized English title of each movie in each line in the form of
 "movie name" (release_year) with NO extra words or sentences.
 1046
 1047 Here is the conversation: {context}

1048 D.2 BASELINES USED IN THE MAIN PAPER

- 1051 • **Redial** (Li et al., 2018) employs a denoising autoencoder to model user-mentioned items and
 1052 generate recommendations, while simultaneously using an recurrent neural network (RNN)-based
 1053 architecture to model and produce conversational utterances.
- 1054 • **KBRD** (Chen et al., 2019) augments CRS with external knowledge graphs. It applies a rela-
 1055 tional graph neural network (RGNN) over the DBpedia knowledge graph to encode entities and
 1056 maximizes the similarity between co-occurring words and entities, thereby fusing semantic and
 1057 knowledge-level signals for recommendation.
- 1058 • **KGSF** (Zhou et al., 2020) further extends knowledge-enhanced CRS by integrating a word-level
 1059 KG (from ConceptNet) into conversations. It leverages mutual information maximization between
 1060 conversational semantics and entity KG embeddings to fuse entity information at the word level.
- 1061 • **UniCRS** (Wang et al., 2022) introduces a unified pre-trained transformer backbone to capture
 1062 dialogue context, with a cross-attention mechanism over entity embeddings learned from RGNN.
 1063 This enables the model to fuse knowledge graph information with conversational semantics.
- 1064 • **Zero-shot LLM** (He et al., 2023) applies large language models directly to CRS. Dialogues are
 1065 input with task-specific prompts and formatting instructions to elicit recommendation lists, but
 1066 without grounding to a catalog or augmenting with external retrieval.
- 1067 • **NBCRS** (Xie et al., 2024) uses Sentence-BERT to retrieve training conversations similar to a
 1068 given test conversation and takes the majority vote of the groundtruth items as recommendations.
 1069 Neighbor size is selected based on the validation set.
- 1070 • **CRAG** (Zhu et al., 2025) retrieves collaborative knowledge based on mentioned items and his-
 1071 torical user-item interactions. Specifically, it introduces a two-step reflection mechanism with
 1072 LLM-as-a-judge to refine the retrieved items and the final ranking.

1074 D.3 ADDITIONAL COMPARISON WITH RL-FREE POST-TRAINING-BASED METHODS

1076 In this part, we compare Rank-GRPO with several RL-free post-training methods for LLM-based
 1077 recommender systems based on direct preference optimization (DPO) (Rafailov et al., 2023). DPO
 1078 assumes access to pairwise preferences over responses to the same prompt and shows that, under a
 1079 Bradley–Terry model (Bradley & Terry, 1952) for the latent reward, a simple maximum-likelihood
 objective can be derived to directly optimize the policy π_θ from preference data. Due to the pairwise

1080
 1081 Table 3: Comparison between ConvRec-R1 and various DPO-based RL-free preference alignment
 1082 baselines with different backbone models on the REDDIT-v2 dataset.

Method	R@5	R@10	R@15	R@20	N@5	N@10	N@15	N@20
Qwen2.5-0.5B (zero-shot)	0.0021	0.0021	0.0021	0.0021	0.0023	0.0022	0.0021	0.0021
+ SFT (DPO) + DPO	0.0716	0.1058	0.1300	0.1473	0.0570	0.0681	0.0752	0.0797
+ SFT (DPO) + S-DPO	0.0875	0.1240	0.1488	0.1699	0.0657	0.0772	0.0845	0.0888
+ SFT (DPO) + SPRec	0.0841	0.1256	0.1524	0.1686	0.0657	0.0775	0.0855	0.0898
+ SFT + Rank-GRPO (\exp_{∞})	0.0946	0.1468	0.1813	0.2047	0.0744	0.0915	0.1016	0.1079
LLama-3.2-1B (zero-shot)	0.0187	0.0240	0.0257	0.0263	0.0157	0.0170	0.0175	0.0176
+ SFT (DPO) + DPO	0.0823	0.1158	0.1437	0.1636	0.0646	0.0752	0.0834	0.0887
+ SFT (DPO) + S-DPO	0.0904	0.1307	0.1588	0.1860	0.0718	0.0829	0.0926	0.0987
+ SFT (DPO) + SPRec	0.0928	0.1375	0.1591	0.1889	0.0758	0.0887	0.0953	0.1050
+ SFT + Rank-GRPO (\exp_{∞})	0.1039	0.1569	0.1937	0.2165	0.0813	0.0985	0.1092	0.1153
LLama-3.2-3B (zero-shot)	0.0574	0.0805	0.0912	0.0961	0.0463	0.0535	0.0566	0.0580
+ SFT (DPO) + DPO	0.0894	0.1279	0.1491	0.1697	0.0708	0.0808	0.0915	0.0896
+ SFT (DPO) + S-DPO	0.1072	0.1419	0.1734	0.1943	0.0807	0.0933	0.1019	0.1079
+ SFT (DPO) + SPRec	0.1053	0.1491	0.1809	0.1965	0.0828	0.0956	0.1043	0.1109
+ SFT + Rank-GRPO (\exp_{∞})	0.1178	0.1756	0.2150	0.2368	0.0919	0.1107	0.1223	0.1283

1098
 1099
 1100 comparison nature of DPO (where it is difficult to define preference between two ranked lists),
 1101 existing DPO variants for recommendation are primarily designed for *candidate-selection* scenarios,
 1102 i.e., choosing positive items from a small candidate set given in the prompt (Wu et al., 2025). In
 1103 contrast, Rank-GRPO targets a more *generative* setting, where a ranked list of N items is generated
 1104 directly by the LLM-based policy based on the conversational context, removing the need for an
 1105 explicit retriever. In addition to the vanilla DPO, the DPO-based baselines considered are as follows:

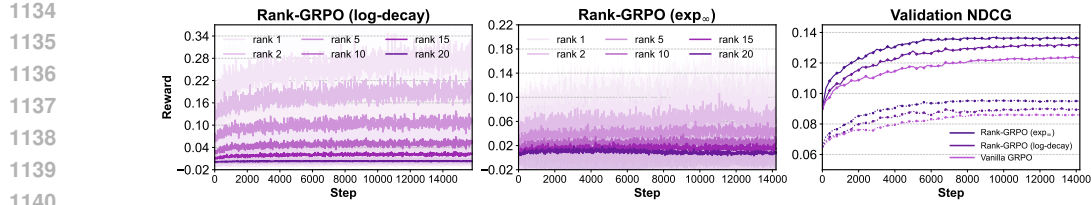
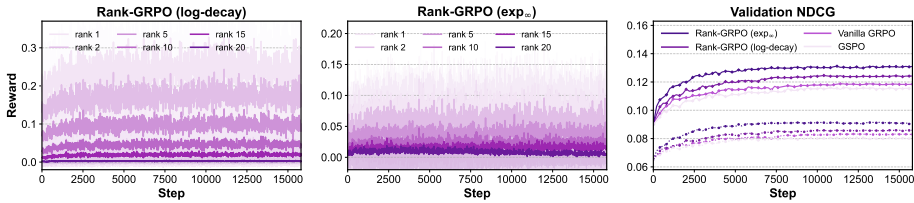
1106 • **S-DPO** (Chen et al., 2024) extends DPO to *multiple* negatives in the candidate set and optimizes
 1107 a softmax-based DPO loss over one preferred item and several dispreferred items.

1108 • **SPRec** (Gao et al., 2025) builds on S-DPO with a self-play procedure that alternates SFT on pos-
 1109 itive items and DPO steps where negatives are drawn from the model’s own previous predictions.

1111 During training, we first perform an SFT (DPO) phase, where we modify the prompt used in Rank-
 1112 GRPO (see Section D.1) to request only a *single* recommendation, and use the ground-truth items
 1113 as supervision. We find this setup substantially improves performance for DPO-based methods
 1114 compared to directly using ranked-list data for SFT (as with ConvRec-R1). To adapt vanilla DPO
 1115 and S-DPO to the generative ranking setting studied in this paper, we follow SPRec (Gao et al.,
 1116 2025) and adopt BIGRec (Bao et al., 2025) to score items and induce a full ranking over the catalog.
 1117 Even though we cache a shared prefix for the conversational context, this pipeline is still slower
 1118 than ConvRec-R1, as it needs to score a large number of catalog items. Empirically, as shown in
 1119 Table 3, both vanilla DPO and its extensions (S-DPO and SPRec) significantly improve upon the
 1120 zero-shot model. However, there remains a gap between these adapted DPO variants and Rank-
 1121 GRPO. This highlights the advantage of Rank-GRPO for *generative* ranking: the model directly
 1122 produces a ranked list by jointly considering the context and previously generated items, rather than
 1123 relying on post-hoc ranking from per-item scores. At the same time, we emphasize that DPO and S-
 1124 DPO are not originally designed for generative ranking tasks; they remain strong RL-free baselines
 1125 when a high-quality retriever is available to propose a compact candidate set in the prompt.

1126 D.4 ADDITIONAL RESULTS FOR THE LLAMA3.2-1B MODEL

1128 In this section, we provide the training dynamics of ConvRec-R1 with **LLama3.2-1B-Instruct** model
 1129 as the backbone under the **on/off-policy** setting, as illustrated in Figs. 4, 5. The results mirror the
 1130 observations from smaller and larger backbones in Section 3.4: (i) training rewards increase con-
 1131 sistently across ranks, confirming that Rank-GRPO enables more stable credit assignment even in
 1132 mid-sized models; (ii) validation NDCG improves more rapidly than with vanilla GRPO, indicating
 1133 that the rank-level importance weighting contributes to faster convergence; and (iii) improvements
 accumulate particularly toward the tail positions of the list, where methods with sequence-level re-

Figure 4: Training dynamics of ConvRec-R1 with **Llama3.2-1B-Instruct** backbone (on-policy).Figure 5: Comparison of training dynamics of reward and validation NDCG between GRPO, GSPO and Rank-GRPO (**off-policy**) with **Llama3.2-1B-Instruct** backbone on the REDDIT-V2 dataset.

ward typically degrade. These dynamics highlight that the advantages of Rank-GRPO generalize across backbone sizes, striking a balance between training efficiency and model capacity.

D.5 TEST SET EVALUATION RESULTS FOR THE OFF-POLICY SETTING

Table 4 presents the test set performance of ConvRec-R1 and baselines under the off-policy setting ($\mu = 2$). As expected, all methods perform worse than their on-policy counterparts in Table ??, reflecting the additional variance introduced by importance weighting. Nevertheless, Rank-GRPO consistently outperforms both vanilla GRPO and GSPO across nearly all metrics, delivering the most substantial improvements over the SFT baseline. These results highlight that, although off-policy training is inherently more challenging for RL-based post-training, the use of rank-level importance weighting enables more stable and effective updates than sequence- or token-level approaches. Consequently, ConvRec-R1 maintains strong recommendation quality (compared with GPT-4o and GPT-4o-mini) while benefiting from the efficiency of reusing previously sampled trajectories.

D.6 ADDITIONAL ANALYSIS OF CATALOG MEMORIZATION DURING THE RL SETTING

To further evaluate the impact of RL on catalog grounding, we track the catalog hit ratio on the validation set throughout training (Figure 6). We find that the recommendations from both GRPO and Rank-GRPO gradually drift away from the catalog as training progresses, due to the absence of direct catalog grounding as in the SFT stage. However, the drift is noticeably slower for Rank-GRPO, since its rank-level return explicitly assigns zero reward in-position to out-of-catalog items, whereas GRPO struggles with proper credit assignment with the sequence-level reward. An additional artifact is observed when comparing backbone sizes: the 0.5B model exhibits stronger fluctuations in the in-catalog ratio, while the 3B model yields a smoother curve. This difference stems from our stabilization strategy: on larger models (1B and 3B), we reduce the learning rate in the second epoch to prevent vanilla GRPO from collapsing (we use the same learning rate on Rank-GRPO for fairness of comparison), whereas the 0.5B model remains stable with 1×10^{-6} .

D.7 ADDITIONAL RESULTS ON THE REDIAL DATASET

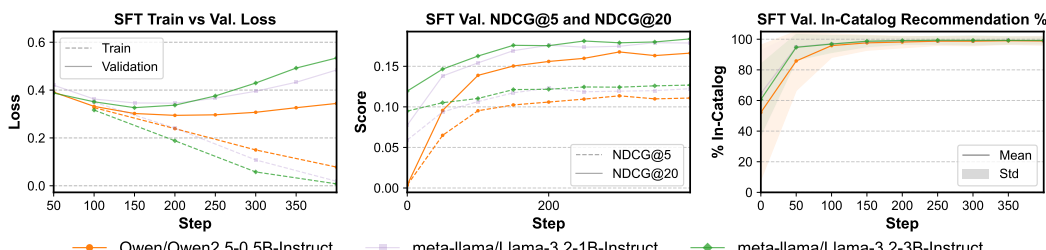
In this section, we present experiments on the REDIAL dataset (Li et al., 2018). Compared to the REDDIT-V2 dataset reported in the main paper, the REDIAL dataset is smaller in scale, with fewer conversations and a smaller movie catalog. It consists of multi-turn dialogues between a seeker and a recommender, where the seeker describes their preferences and the recommender suggests movies in natural language. We follow the standard split protocol: 80% for training (20,896 conversations),

1188

1189 Table 4: Comparison between ConvRec-R1 and various baselines on the REDDIT-V2 dataset in the
1190 **off-policy** setting. Here, R@ k and N@ k stand for Recall@ k and NDCG@ k , respectively.

1191

Method	R@5	R@10	R@15	R@20	N@5	N@10	N@15	N@20
Traditional and Transformer-based CRS								
Redial (Li et al., 2018)	0.0103	0.0228	0.0274	0.0322	0.0073	0.0113	0.0128	0.0143
KBRD (Chen et al., 2019)	0.0444	0.0813	0.1058	0.1223	0.0305	0.0418	0.0490	0.0545
KGSF (Zhou et al., 2020)	0.0579	0.0921	0.1246	0.1433	0.0405	0.0503	0.0599	0.0662
UniCRS (Wang et al., 2022)	0.0722	0.1053	0.1344	0.1494	0.0548	0.0640	0.0726	0.0778
NBCRS (Xie et al., 2024)	0.0801	0.1290	0.1655	0.2019	0.0661	0.0833	0.0954	0.1048
LLM Prompting-Based Methods								
GPT-4o-mini (zero-shot)	0.0949	0.1348	0.1600	0.1687	0.0747	0.0877	0.0950	0.0973
GPT-4o (zero-shot) (He et al., 2023)	0.1106	0.1625	0.1992	0.2147	0.0861	0.1028	0.1136	0.1197
CRAG (Zhu et al. (2025))	0.1146	0.1715	0.2030	0.2212	0.0885	0.1065	0.1164	0.1227
LLM Post-Training-Based Methods (off-policy, $\mu = 2$)								
Most results are significant as standard error are between 0.0020-0.0035 for R@5-20 and 0.0015-0.0025 for N@5-20								
Qwen2.5-0.5B (zero-shot)	0.0021	0.0021	0.0021	0.0021	0.0023	0.0022	0.0021	0.0021
+ SFT	0.0642	0.1027	0.1212	0.1308	0.0502	0.0625	0.0678	0.0704
+ SFT+Vanilla GRPO	0.0781	0.1176	0.1429	0.1538	0.0623	0.0748	0.0823	0.0852
+ SFT+ GSPO	0.0816	0.1243	0.1511	0.1641	0.0647	0.0784	0.0862	0.0896
+ SFT+Rank-GRPO (log)	0.0818	0.1256	0.1604	0.1764	0.0644	0.0784	0.0886	0.0930
+ SFT+Rank-GRPO (\exp_{∞})	0.0935	0.1412	0.1738	0.1899	0.0735	0.0887	0.0982	0.1025
Llama-3.2-1B (zero-shot)	0.0187	0.0240	0.0257	0.0263	0.0157	0.0170	0.0175	0.0176
+ SFT	0.0754	0.1148	0.1354	0.1498	0.0595	0.0723	0.0782	0.0819
+ SFT+Vanilla GRPO	0.0937	0.1415	0.1726	0.1974	0.0728	0.0882	0.0975	0.1042
+ SFT+GSPO	0.0901	0.1389	0.1693	0.1899	0.0700	0.0857	0.0947	0.1002
+ SFT+Rank-GRPO (log)	0.0937	0.1464	0.1832	0.2066	0.0731	0.0902	0.1011	0.1074
+ SFT+Rank-GRPO (\exp_{∞})	0.1037	0.1555	0.1927	0.2166	0.0806	0.0973	0.1081	0.1146
Llama-3.2-3B (zero-shot)	0.0574	0.0805	0.0912	0.0961	0.0463	0.0535	0.0566	0.0580
+ SFT	0.0788	0.1191	0.1410	0.1541	0.0615	0.0744	0.0807	0.0842
+ SFT+Vanilla GRPO	0.0952	0.1425	0.1726	0.1952	0.0766	0.0916	0.1004	0.1065
+ SFT+GSPO	0.0942	0.1436	0.1770	0.1943	0.0758	0.0914	0.1011	0.1058
+ SFT+Rank-GRPO (log)	0.1037	0.1572	0.1958	0.2220	0.0816	0.0989	0.1101	0.1169
+ SFT+Rank-GRPO (\exp_{∞})	0.1092	0.1653	0.2010	0.2272	0.0845	0.1028	0.1132	0.1203

1228 Figure 7: Training dynamics on loss, validation metrics, validation in-catalog recommendation ratio
1229 with different backbone models during the **SFT** stage on the REDIAL dataset.1230
1231 10% for validation (2,612), and 10% for testing (2,613) (He et al., 2023). In addition, we choose
1232 a different teacher model, i.e., Claude-3.7-Sonnet, to demonstrate the generalization over different
1233 large teacher LLM to generate the catalog-grounded behavior cloning dataset.
12341235

D.7.1 EVALUATION ON THE SFT STAGE

 12361237 As shown in Fig. 7, as with the results on the REDDIT-V2 dataset (see Section 3.3), training loss
1238 decreases steadily, while validation loss quickly plateaus, reflecting the difficulty of direct imitation
1239 learning when the outputs from teachers are long, structured recommendation lists. At the same time,
1240 the in-catalog recommendation ratio rapidly approaches nearly 100% across all three backbones,
1241 indicating that the Remap–Reflect–Adjust pipeline plus SFT is effective at grounding the models in
the Redial catalog. Finally, NDCG@20 on the validation set improves substantially over the zero-

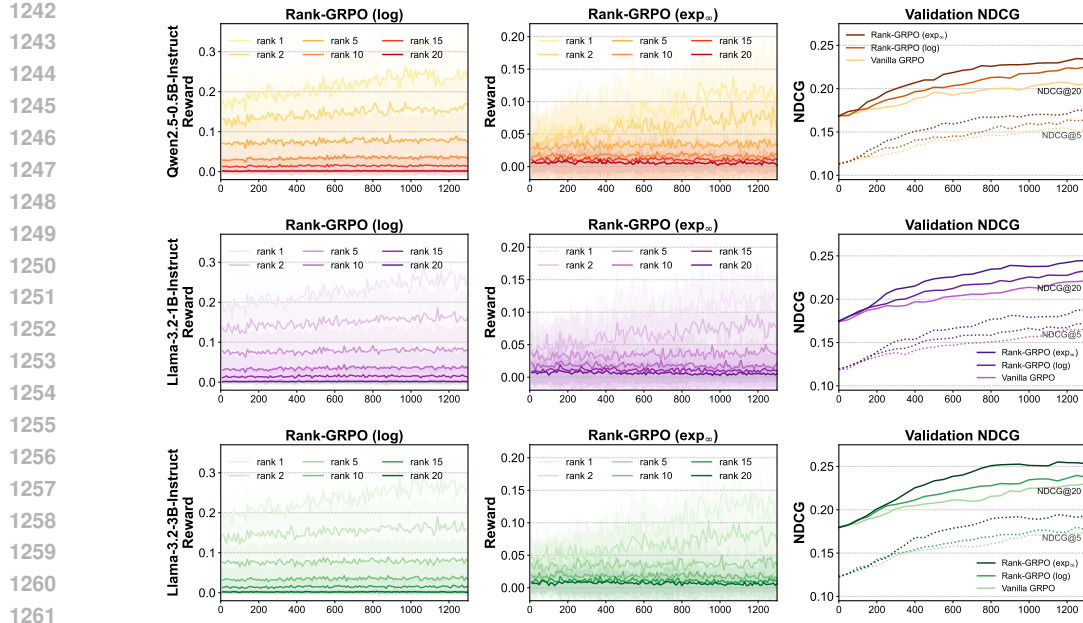


Figure 8: **Left + Middle:** Training dynamics of the reward acquired by ConvRec-R1 with Rank-GRPO on different rank during the **RL** stage. **Right:** Comparison of validation NDCG between GRPO and Rank-GRPO (both on-policy) on the REDIAL dataset.

Table 5: Comparison between ConvRec-R1 and various baselines on the REDIAL dataset in the on-policy setting. Here, R@ k and N@ k stand for Recall@ k and NDCG@ k , respectively.

Method	R@5	R@10	R@15	R@20	N@5	N@10	N@15	N@20
Traditional and Transformer-based CRS								
Redial (Li et al., 2018)	0.0178	0.0380	0.0440	0.0502	0.0114	0.0187	0.0203	0.0221
KBRD (Chen et al., 2019)	0.0763	0.1356	0.1697	0.1907	0.0474	0.0686	0.0778	0.0840
KGSF (Zhou et al., 2020)	0.0995	0.1535	0.1999	0.2235	0.0630	0.0826	0.0951	0.1020
UniCRS (Wang et al., 2022)	0.1241	0.1756	0.2156	0.2330	0.0851	0.1050	0.1153	0.1199
NBCRS (Xie et al., 2024)	0.1848	0.2874	0.3687	0.4108	0.1228	0.1568	0.1788	0.1891
LLM Prompting-Based Methods								
Claude-3.7 (zero-shot) (He et al., 2023)	0.2088	0.3135	0.3717	0.4097	0.1346	0.1691	0.1849	0.1941
CRAG (Zhu et al., 2025)	0.2097	0.3211	0.3810	0.4201	0.1300	0.1720	0.1889	0.1976
LLM RL Post-Training-Based Methods								
Qwen2.5-0.5B (zero-shot)	0.0050	0.0050	0.0050	0.0050	0.0042	0.0042	0.0042	0.0042
+ SFT	0.1634	0.2570	0.3145	0.3512	0.1036	0.1345	0.1502	0.1590
+ SFT+Vanilla GRPO	0.2114	0.3095	0.3633	0.3917	0.1431	0.1756	0.1902	0.1971
+ SFT+Rank-GRPO (log)	0.2251	0.3253	0.3885	0.4272	0.1531	0.1857	0.2029	0.2123
+ SFT+Rank-GRPO (\exp_{∞})	0.2385	0.3542	0.4153	0.4431	0.1640	0.2018	0.2184	0.2252
Llama-3.2-1B (zero-shot)	0.1036	0.1522	0.1672	0.1704	0.0657	0.0818	0.0859	0.0867
+ SFT	0.1714	0.2731	0.3345	0.3715	0.1078	0.1414	0.1580	0.1671
+ SFT+Vanilla GRPO	0.2236	0.3296	0.3924	0.4196	0.1526	0.1876	0.2047	0.2114
+ SFT+Rank-GRPO (log)	0.2365	0.3392	0.4059	0.4472	0.1605	0.1942	0.2125	0.2226
+ SFT+Rank-GRPO (\exp_{∞})	0.2516	0.3651	0.4255	0.4526	0.1714	0.2092	0.2257	0.2323
Llama-3.2-3B (zero-shot)	0.1473	0.2030	0.2284	0.2309	0.0972	0.1158	0.1228	0.1234
+ SFT	0.1756	0.2750	0.3392	0.3793	0.1114	0.1441	0.1615	0.1712
+ SFT+Vanilla GRPO	0.2282	0.3265	0.3936	0.4300	0.1574	0.1898	0.2080	0.2168
+ SFT+Rank-GRPO (log)	0.2378	0.3391	0.4084	0.4471	0.1630	0.1964	0.2153	0.2247
+ SFT+Rank-GRPO (\exp_{∞})	0.2691	0.3740	0.4361	0.4648	0.1820	0.2167	0.2336	0.2405

shot models, confirming that SFT again provides a strong warm start for the subsequent RL stage by bestowing the backbone LLM with preliminary generative ranking abilities.

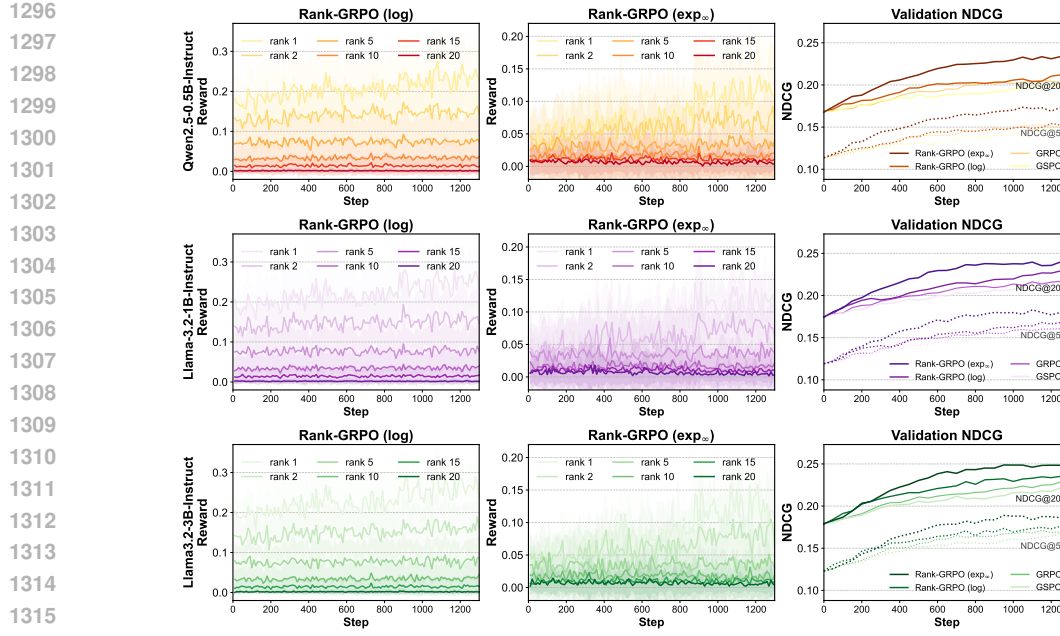


Figure 9: **Left + Middle:** Training dynamics of the reward acquired by ConvRec-R1 with Rank-GRPO on different rank during the **RL** stage. **Right:** Comparison of validation NDCG between GRPO and Rank-GRPO (**off-policy**) on the REDIAL dataset.

D.7.2 EVALUATION ON THE RL STAGE

On the RL stage, we also observe similar trends to the results on REDDIT-V2 (Section 3.4). In the on-policy setting (left and middle panels of Fig. 8), the rank-wise rewards under Rank-GRPO increase across ranks, indicating the ability of ConvRec-R1 to improve the entire recommendation list. The right panel shows that Rank-GRPO consistently converges to higher validation NDCG than vanilla GRPO for all three backbones, with the gains being more pronounced at larger k , again suggesting that Rank-GRPO is particularly effective at maintaining quality toward the tail of the list. In the off-policy setting with per-sampling update step $\mu = 2$ (see Fig. 9), Rank-GRPO also compare favorably over GRPO and GSPO in terms of validation NDCG. The off-policy curves lag slightly behind their on-policy counterparts due to the additional variance introduced by importance weighting, but they still achieve clear improvements over the SFT and vanilla GRPO baselines.

Furthermore, Tables 5 and 6 show that on REDIAL, ConvRec-R1 again substantially improves over both zero-shot and SFT-only backbones, and consistently outperforms vanilla GRPO (and GSPO in the off-policy case) across backbones and metrics. The Llama-3.2-3B backbone with Rank-GRPO (\exp_∞) achieves the best overall performance, surpassing both zero-shot Claude-3.7 and a RAG-based LLM system composed of Claude-3.7 with substantially less inference cost.

D.7.3 SENSITIVITY W.R.T. REWARD SHAPING HYPERPARAMETER

In this part, we examine the influence of the reward-shaping hyperparameter introduced in Section 2.3.3. Recall that we add a per-token penalty $\epsilon_o < 0$ to enforce instruction following: premature `<eos>` tokens that stop generation before N items are produced receive a penalty, and any overflow items beyond rank N are also penalized. We sweep $\epsilon_o \in \{0, -0.01, -0.1, -0.5, -1\}$ and train Rank-GRPO (\exp_∞) with the Qwen2.5-0.5B-Instruct backbone; the resulting Recall@K curves are shown in Fig. 10. When no penalty is applied ($\epsilon_o = 0$), performance is noticeably worse, reflecting the fact that failures to respect the required list length are not corrected by the reward signal. In contrast, once

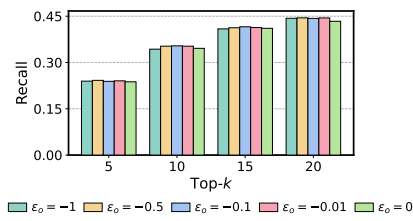


Figure 10: Sensitivity of Recall@ k for Rank-GRPO (\exp_∞) to ϵ_o with Qwen2.5-0.5B-Instruct.

1350
 1351 Table 6: Comparison between ConvRec-R1 and various baselines in the *off-policy* setting on the
 1352 REDIAL dataset. Here, R@ k and N@ k stand for Recall@ k and NDCG@ k , respectively.

Method	R@5	R@10	R@15	R@20	N@5	N@10	N@15	N@20
LLM Post-Training-Based Methods (off-policy, $\mu = 2$)								
Qwen2.5-0.5B (zero-shot)	0.0050	0.0050	0.0050	0.0050	0.0042	0.0042	0.0042	0.0042
+ SFT	0.1634	0.2570	0.3145	0.3512	0.1036	0.1345	0.1502	0.1590
+ SFT+Vanilla GRPO	0.2095	0.3005	0.3506	0.3829	0.1422	0.1720	0.1857	0.1936
+ SFT+GSPO	0.2056	0.3005	0.3536	0.3841	0.1379	0.1692	0.1837	0.1911
+ SFT+Rank-GRPO (log)	0.2140	0.3143	0.3694	0.4038	0.1470	0.1801	0.1950	0.2034
+ SFT+Rank-GRPO (\exp_∞)	0.2363	0.3399	0.3993	0.4350	0.1614	0.1956	0.2118	0.2205
Llama-3.2-1B (zero-shot)	0.1036	0.1522	0.1672	0.1704	0.0657	0.0818	0.0859	0.0867
+ SFT	0.1714	0.2731	0.3345	0.3715	0.1078	0.1414	0.1580	0.1671
+ SFT+Vanilla GRPO	0.2218	0.3255	0.3790	0.4143	0.1495	0.1835	0.1981	0.2066
+ SFT+GSPO	0.2156	0.3102	0.3705	0.4157	0.1438	0.1748	0.1911	0.2022
+ SFT+Rank-GRPO (log)	0.2249	0.3277	0.3910	0.4345	0.1535	0.1874	0.2046	0.2153
+ SFT+Rank-GRPO (\exp_∞)	0.2479	0.3562	0.4225	0.4429	0.1659	0.2020	0.2200	0.2251
Llama-3.2-3B (zero-shot)	0.1473	0.2030	0.2284	0.2309	0.0972	0.1158	0.1228	0.1234
+ SFT	0.1756	0.2750	0.3392	0.3793	0.1114	0.1441	0.1615	0.1712
+ SFT+Vanilla GRPO	0.2237	0.3228	0.3895	0.4268	0.1546	0.1872	0.2053	0.2144
+ SFT+GSPO	0.2242	0.3198	0.3781	0.4188	0.1535	0.1853	0.2012	0.2111
+ SFT+Rank-GRPO (log)	0.2327	0.3404	0.3997	0.4424	0.1620	0.1976	0.2137	0.2240
+ SFT+Rank-GRPO (\exp_∞)	0.2648	0.3713	0.4332	0.4610	0.1792	0.2148	0.2322	0.2385

1371
 1372 Table 7: Comparison between ConvRec-R1 and various baselines on the REDIAL dataset with
 1373 Qwen2.5-7B-Instruct backbone. R@ k and N@ k stand for Recall@ k and NDCG@ k , respectively.

Method	R@5	R@10	R@15	R@20	N@5	N@10	N@15	N@20
Qwen-2.5-7B (zero-shot)	0.1272	0.1913	0.2175	0.2217	0.0795	0.1006	0.1078	0.1088
+ SFT	0.1807	0.2723	0.3342	0.3703	0.1164	0.1465	0.1636	0.1723
+ SFT+Vanilla GRPO	0.2286	0.3288	0.3753	0.4207	0.1516	0.1879	0.2019	0.2095
+ SFT+Rank-GRPO (log)	0.2415	0.3491	0.4012	0.4495	0.1646	0.1986	0.2176	0.2245
+ SFT+Rank-GRPO (\exp_∞)	0.2723	0.3764	0.4427	0.4745	0.1811	0.2158	0.2338	0.2416

1381 any negative penalty is introduced, the performance first increases and then decreases when ϵ_o de-
 1382 creases from -0.01 to 1 , but the fluctuation is not very significant. This indicates that performance
 1383 of Rank-GRPO is quite robust to the exact magnitude of the penalty, with only mild fluctuations.

D.7.4 GENERALIZATION TO LARGER MODELS

1384
 1385 Although in practice, we expect models with up to 3B parameters to be the most suitable for the real-
 1386 world deployment of CRS due to latency and memory constraints, we also conduct an exploratory
 1387 study with a larger backbone to assess the scalability of ConvRec-R1 and Rank-GRPO. Specifically,
 1388 Table 7 reports additional results on the REDIAL dataset with the Qwen2.5-7B-Instruct backbone.
 1389 Training this 7B model on the full REDDIT-v2 dataset ($\sim 400k$ conversations) is beyond our current
 1390 computational budget, so we only experiment on the smaller REDIAL benchmark. Notably, we
 1391 observe trends that are consistent with those of smaller models: SFT provides a strong improvement
 1392 over the zero-shot baseline, and Rank-GRPO further boosts the ranking ability of the LLM. In
 1393 particular, the Qwen2.5-7B-Instruct + Rank-GRPO (\exp_∞) model slightly surpasses the Llama-3.2-
 1394 3B-Instruct counterpart on most metrics (see Table 5). These findings suggest that ConvRec-R1 and
 1395 Rank-GRPO generalize well to larger backbones when computational resources permit.

D.8 ANALYSIS OF IN-CATALOG RATE AFTER THE RL STAGE

1396
 1397 In Table 8, we report the in-catalog ratios of recommendations generated with ConvRec-R1 after the
 1398 Rank-GRPO stage on both the REDDIT-v2 and REDIAL datasets, under on-policy and off-policy
 1399 training settings. Across all backbones, we note that the model maintains very high catalog validity:
 1400 over 98% of generated items are in-catalog on REDDIT-v2 and typically between 95–99% on RE-
 1401 DIAL. Since out-of-catalog titles are already rare at this point, a deployed system can either reuse the
 1402 1403

1404
1405
1406

Table 8: In-catalog ratios (%) of recommendations generated by ConvRec-R1 after the Rank-GRPO stage on the REDDIT-V2 and REDIAL datasets.

1407
1408
1409
1410
1411
1412

Dataset	Setting	Qwen2.5-0.5B	Llama-3.2-1B	Llama-3.2-3B
REDDIT-V2	On-policy	99.61 \pm 1.50	98.40 \pm 3.76	99.46 \pm 1.77
	Off-policy	98.52 \pm 3.21	98.51 \pm 3.31	99.50 \pm 1.76
REDIAL	On-policy	97.77 \pm 3.71	98.12 \pm 3.72	98.53 \pm 3.12
	Off-policy	97.93 \pm 3.60	95.52 \pm 5.41	97.82 \pm 4.30

1413

1414 Remap step from the SFT pipeline to map such outputs to the nearest valid catalog item, or simply
1415 filter them out, effectively eliminating residual out-of-catalog drift in practice.
14161417
1418

E DISCUSSION ON GENERALIZATION OF CONVREC-R1

1419
1420
1421
1422
1423
1424
1425
1426
1427
1428
1429
1430
1431
1432

There are three main datasets widely used in CRS research, i.e., REDDIT-V2 (He et al., 2023; Zhu et al., 2025), REDIAL (Li et al., 2018), and INSPIRE (Hayati et al., 2020), all focused on movie recommendations. We exclude INSPIRE from experiments because it contains only 1,000 conversations, which is insufficient to reliably fine-tune LLMs with billions of parameters. An advantage of the movie recommendation setting is that each item (movie) naturally comes with a short textual representation (e.g., title with release year), which can be understood by the LLM and directly used as the item tokens. To generalize ConvRec-R1 to other domains such as e-commerce or short-video recommendation, we can either use pretrained textual tokens (Hou et al., 2024; Zhang et al., 2025a) or introduce new special tokens (Zhu et al., 2024b; Hua et al., 2023) as a codebook to represent items. However, since not all arbitrary token combinations in the codebook correspond to valid items, the proposed SFT stage with *reflect-rank-adjust* can still be applied to teach the LLM catalog awareness and to endow it with preliminary generative ranking ability over a predefined item catalog. The subsequent RL stage with Rank-GRPO can then be applied to utilize the verifiable, rank-wise rewards defined over the generated items to align the generations with user preferences.

1433
1434
1435
1436
1437
1438
1439
1440
1441
1442
1443
1444
1445
1446
1447
1448
1449
1450
1451
1452
1453
1454
1455
1456
1457

1458 F QUALITATIVE EXAMPLES
1459

1460 Comparison between Zero-Shot and SFT/RL stage of ConvRec-R1 with Qwen2.5-0.5B		
1461	(i) Conversation x_i^{SFT} :	
1462	1463 User: Best 3d movies to watch?. What are the best 3d movies to watch on my vr headset (except Avatar and mcu movies)? I want the 3d effects to actually be good and not some cheap garbage 3d processing some studios apply to their movies. I also want the 3d to actually be immersive and cool. Movies I have already seen in 3d are: Avatar, avengers, godzilla, star wars the force awakens, pixels, terminator genesys and jurassic world.	1464
1465	1466	1467
1468	1469 Groundtruth y_i^{gt}: Terminator 2: Judgment Day (1991), Hugo (2011), The Walk (2015), Titanic (1997), Ready Player One (2018), Predator (1987), Jurassic Park (1993), Mad Max: Fury Road (2015), Kong: Skull Island (2017), Gravity (2013), Life of Pi (2012), Blade Runner 2049 (2017), Pacific Rim (2013)	1470
1471	(iii) Outputs from Qwen2.5-0.5B:	
1472	Rk. (a) Zero-Shot Raw Output	Processed Rec. (NDCG@20=0.000)
1473	1474 1 Avatar	Avatar
1475	2 Avengers	Avengers
1476	3 Godzilla	Godzilla
1477	4 Star Wars: The Force Awakens	Star Wars: The Force Awakens
1478	5 Pixels	Pixels
1479	6 Terminator: Genesys	Terminator: Genesys
1480	7 Jurassic World	Jurassic World
1481	Rk. (b) After SFT (Checkpoint-1500) Raw Output	Processed Rec. (NDCG@20=0.249, 0.249 ▲)
1482	1 Guardians of the Galaxy (2014)	Guardians of the Galaxy (2014)
1483	2 Mad Max: Fury Road (2015)	Mad Max: Fury Road (2015)
1484	3 The Jungle Book (2016)	The Jungle Book (2016)
1485	4 Interstellar (2014)	Interstellar (2014)
1486	5 Gravity (2013)	Gravity (2013)
1487	6 Inception (2010)	Inception (2010)
1488	7 The Matrix (1999)	The Matrix (1999)
1489	8 Ready Player One (2018)	Ready Player One (2018)
1490	9 Oblivion (2013)	Oblivion (2013)
1491	10 The Dark Knight Rises (2012)	The Dark Knight Rises (2012)
1492	11 The Adventures of Tintin (2011)	The Adventures of Tintin (2011)
1493	12 Tron: Legacy (2010)	Tron: Legacy (2010)
1494	13 Valerian and City of a Thousand Planets (2017)	Valerian and City of a Thousand Planets (2017)
1495	14 The Fifth Element (1997)	The Fifth Element (1997)
1496	15 Jumanji: Welcome to the Jungle (2017)	Jumanji: Welcome to the Jungle (2017)
1497	16 The Last of Us (2013)	The Last of Us (2013)
1498	17 The Hobbit: An Unexpected Journey (2012)	The Hobbit: An Unexpected Journey (2012)
1499	...	
1500	Rk. (c) After RL (Checkpoint-15800) Raw Output	Processed Rec. (NDCG@20=0.444, 0.195 ▲)
1501	1 Mad Max: Fury Road (2015)	Mad Max: Fury Road (2015)
1502	2 Interstellar (2014)	Interstellar (2014)
1503	3 The Matrix (1999)	The Matrix (1999)
1504	4 Blade Runner 2049 (2017)	Blade Runner 2049 (2017)
1505	5 Gravity (2013)	Gravity (2013)
1506	6 Inception (2010)	Inception (2010)
1507	7 Ready Player One (2018)	Ready Player One (2018)
1508	8 Guardians of the Galaxy (2014)	Guardians of the Galaxy (2014)
1509	9 Alita: Battle Angel (2019)	Alita: Battle Angel (2019)
1510	10 Tron: Legacy (2010)	Tron: Legacy (2010)
1511	11 The Fifth Element (1997)	The Fifth Element (1997)
1512	12 Ready or Not (2019)	Ready or Not (2019)
1513	13 Valerian and City of a Thousand Planets (2017)	Valerian and City of a Thousand Planets (2017)
1514	14 Edge of Tomorrow (2014)	Edge of Tomorrow (2014)
1515	15 Oblivion (2013)	Oblivion (2013)
1516	16 The Dark Knight Rises (2012)	The Dark Knight Rises (2012)
1517	17 Dunkirk (2017)	Dunkirk (2017)
1518	...	

1512

1513 **Comparison between Zero-Shot and SFT/RL stage of ConvRec-R1 with Llama-3.2-1B**

1514

(i) Conversation x_i^{SFT} :

1515

>User: Best 3d movies to watch?. What are the best 3d movies to watch on my vr headset (except Avatar and mcu movies)? I want the 3d effects to actually be good and not some cheap garbage 3d processing some studios apply to their movies. I also want the 3d to actually be immersive and cool. Movies I have already seen in 3d are: Avatar, avengers, godzilla, star wars the force awakens, pixels, terminator genesys and jurassic world.

1516

1517

1518

1519

1520

1521

1522

1523

(ii) Groundtruth y_i^{gt} : Terminator 2: Judgment Day (1991), Hugo (2011), The Walk (2015), Titanic (1997), Ready Player One (2018), Predator (1987), Jurassic Park (1993), Mad Max: Fury Road (2015), Kong: Skull Island (2017), Gravity (2013), Life of Pi (2012), Blade Runner 2049 (2017), Pacific Rim (2013)

(iii) Outputs from Llama-3.2-1B:

1524

Rk. | (a) Zero-Shot Raw Output

| Processed Rec. (NDCG@20=0.000)

Rk.	Raw Output	Processed Rec. (NDCG@20=0.000)
1	Inception (2010)	Inception (2010)
2	Interstellar (2014)	Interstellar (2014)
3	The Matrix (1999)	The Matrix (1999)
4	The Prestige (2006)	The Prestige (2006)
5	The Lord of the Rings (2001)	The Lord of the Rings (2001)
6	The Dark Knight (2008)	The Dark Knight (2008)
7	The Bourne Identity (2002)	The Bourne Identity (2002)
8-20	(repeats The Prestige)	(repeats The Prestige)

Rk. | (b) After SFT (Checkpoint-1500) Raw Output | Processed Rec. (NDCG@20=0.342, 0.342 ▲)

Rk.	Raw Output	Processed Rec. (NDCG@20=0.342, 0.342 ▲)
1	Blade Runner 2049 (2017)	Blade Runner 2049 (2017)
2	Inception (2010)	Inception (2010)
3	Gravity (2013)	Gravity (2013)
4	The Matrix (1999)	The Matrix (1999)
5	Interstellar (2014)	Interstellar (2014)
6	Dunkirk (2017)	Dunkirk (2017)
7	Ready Player One (2018)	Ready Player One (2018)
8	Alita: Battle Angel (2019)	Alita: Battle Angel (2019)
9	Valerian and City of a Thousand Planets (2017)	Valerian and City of a Thousand Planets (2017)
10	Tron: Legacy (2010)	Tron: Legacy (2010)
11	Jupiter Ascending (2015)	Jupiter Ascending (2015)
12	Guardians of the Galaxy (2014)	Guardians of the Galaxy (2014)
13	Rogue One: A Star Wars Story (2016)	Rogue One: A Star Wars Story (2016)
14	The Final Cut (2004)	The Final Cut (2004)
15	The Green Inferno (2013)	The Green Inferno (2013)
16	The Thirteenth Floor (1999)	The Thirteenth Floor (1999)
17	War for the Planet of the Apes (2017)	War for the Planet of the Apes (2017)
18	The Lord of the Rings (1978)	The Lord of the Rings (1978)

...

Rk. | (c) After RL (Checkpoint-15800) Raw Output | Processed Rec. (NDCG@20=0.129, 0.471 ▲)

Rk.	Raw Output	Processed Rec. (NDCG@20=0.129, 0.471 ▲)
1	Gravity (2013)	Gravity (2013)
2	Blade Runner 2049 (2017)	Blade Runner 2049 (2017)
3	The Matrix (1999)	The Matrix (1999)
4	Alita: Battle Angel (2019)	Alita: Battle Angel (2019)
5	Ready Player One (2018)	Ready Player One (2018)
6	Tron: Legacy (2010)	Tron: Legacy (2010)
7	Valerian and City of a Thousand Planets (2017)	Valerian and City of a Thousand Planets (2017)
8	Rogue One: A Star Wars Story (2016)	Rogue One: A Star Wars Story (2016)
9	Inception (2010)	Inception (2010)
10	Guardians of the Galaxy (2014)	Guardians of the Galaxy (2014)
11	Interstellar (2014)	Interstellar (2014)
12	Jaws (1975)	Jaws (1975)
13	Pacific Rim (2013)	Pacific Rim (2013)
14	War for the Planet of the Apes (2017)	War for the Planet of the Apes (2017)
15	A Nightmare on Elm Street 3 (1987)	A Nightmare on Elm Street 3 (1987)
16	Blade Runner (1982)	Blade Runner (1982)
17	Life of Pi (2012)	Life of Pi (2012)
18	Edge of Tomorrow (2014)	Edge of Tomorrow (2014)

...

1566

1567 **Comparison between Zero-Shot and SFT/RL stage of ConvRec-R1 with Llama-3.2-3B**

1568

(i) Conversation x_i^{SFT} :

1569

User: Best 3d movies to watch?. What are the best 3d movies to watch on my vr headset
(except Avatar and mcu movies)? I want the 3d effects to actually be good and not some cheap
garbage 3d processing some studios apply to their movies. I also want the 3d to actually be
immersive and cool. Movies I have already seen in 3d are: Avatar, avengers, godzilla, star wars
the force awakens, pixels, terminator genesys and jurassic world.

1570

1571

1572

1573

1574

1575

(ii) Groundtruth y_i^{gt} : Terminator 2: Judgment Day (1991), Hugo (2011), The Walk (2015), Titanic
(1997), Ready Player One (2018), Predator (1987), Jurassic Park (1993), Mad Max: Fury Road
(2015), Kong: Skull Island (2017), Gravity (2013), Life of Pi (2012), Blade Runner 2049 (2017),
Pacific Rim (2013)

1576

1577

(iii) Outputs from Llama-3.2-3B:

1578

Rk. | (a) Zero-Shot Raw Output**| Processed Rec. (nDCG@20=0.147)**

1579

1 Interstellar (2014)	Interstellar (2014)
2 The Martian (2015)	The Martian (2015)
3 Mad Max: Fury Road (2015)	Mad Max: Fury Road (2015)
4 The Jungle Book (2016)	The Jungle Book (2016)
5 Fantastic Beasts and Where to Find Them (2016)	Fantastic Beasts and Where to Find Them (2016)
6 The BFG (2016)	The BFG (2016)
7 Dunkirk (2017)	Dunkirk (2017)
8 Wonder Woman (2017)	Wonder Woman (2017)
9 Justice League (2017)	Justice League (2017)
10 Ready Player One (2018)	Ready Player One (2018)
11 Mission: Impossible - Fallout (2018)	Mission: Impossible - Fallout (2018)
12 Spider-Man: Into the Spider-Verse (2018)	Spider-Man: Into the Spider-Verse (2018)
13 Alita: Battle Angel (2019)	Alita: Battle Angel (2019)
14 Captain Marvel (2019)	Captain Marvel (2019)
15 Godzilla: King of the Monsters (2019)	Godzilla: King of the Monsters (2019)

1591

Rk. | (b) After SFT (Checkpoint-1500) Raw Output**| Processed Rec. (nDCG@20=0.385, 0.238 ▲)**

1592

1 Blade Runner 2049 (2017)	Blade Runner 2049 (2017)
2 Mad Max: Fury Road (2015)	Mad Max: Fury Road (2015)
3 Inception (2010)	Inception (2010)
4 The Revenant (2015)	The Revenant (2015)
5 Interstellar (2014)	Interstellar (2014)
6 Alita: Battle Angel (2019)	Alita: Battle Angel (2019)
7 Dunkirk (2017)	Dunkirk (2017)
8 Gravity (2013)	Gravity (2013)
9 The Fall (2006)	The Fall (2006)
10 The Adventures of Milo and Otis (1986)	The Adventures of Milo and Otis (1986)
11 Tron: Legacy (2010)	Tron: Legacy (2010)
12 Ready Player One (2018)	Ready Player One (2018)
13 The Jungle Book (2016)	The Jungle Book (2016)
14 Shang-Chi and Legend of the Ten Rings (2021)	Shang-Chi and Legend of the Ten Rings (2021)
15 War for the Planet of the Apes (2017)	War for the Planet of the Apes (2017)

1605

Rk. | (c) After RL (Checkpoint-15800) Raw Output**| Processed Rec. (nDCG@20=0.475, 0.237 ▲)**

1606

1 Life of Pi (2012)	Life of Pi (2012)
2 Alita: Battle Angel (2019)	Alita: Battle Angel (2019)
3 Ready Player One (2018)	Ready Player One (2018)
4 The Matrix (1999)	The Matrix (1999)
5 Blade Runner 2049 (2017)	Blade Runner 2049 (2017)
6 Gravity (2013)	Gravity (2013)
7 Interstellar (2014)	Interstellar (2014)
8 Tron: Legacy (2010)	Tron: Legacy (2010)
9 Mad Max: Fury Road (2015)	Mad Max: Fury Road (2015)
10 Dunkirk (2017)	Dunkirk (2017)
11 Valerian and City of a Thousand Planets (2017)	Valerian and City of a Thousand Planets (2017)
12 Inception (2010)	Inception (2010)
13 The Fall (2006)	The Fall (2006)
14 Pan's Labyrinth (2006)	Pan's Labyrinth (2006)
15 Blade Runner (1982)	Blade Runner (1982)

1619